Deltares

SWAN-model Haringvliet-Biesbosch

for BOI2023

SWAN-model Haringvliet-Biesbosch
for BOI2023

Author(s)
Mari Irias Mata
Caroline Gautier

SWAN-model Haringvliet-Biesbosch
for BOI2023

Client	Rijkswaterstaat Water, Verkeer en Leefomgeving
Contact	de heer M. Scholten
References	Action Plan KPP 2021 project; MA07ab 2021 - Hydraulic schematics - fresh and salty
Keywords	waves, model schematization , SWAN, Haringvliet-Biesbosch, BOI

Document data	
Version	1.0
Date	30-03-2022
Project number	11208058-037
Document ID	11208058-037-GEO-0001
Pages	57
Classification	
Status	final

Author(s)

	Marisol Irías Mata	
	Caroline Gautier	

Summary

This report presents the setup of the Haringvliet-Biesbosch SWAN model, called swan-hvbb-hr2023_6-v1a. The model is to be used for performing BOI ('Assessment and Design Instrumentation') production computations.

The curvilinear computational grid is taken from the previous model version (Deltares, 2016). We updated bathymetry and obstacles. The directional resolution is 5°. The model uses SWAN version 41.31A.1 and uses the generic settings as recommended in Deltares (2021a en 2021b). The model uses uniform wind- and water level fields. Currents are not included.

Sixteen test computations were performed for the combinations of high and low wind speed (47 m/s and 10 m/s), high and low water level (NAP+7 m and NAP-1 m) and four directions (67.5°N, 202.5° N, 270°N, 315°N). The computations did not reveal anything notable. Our advice is to maintain a maximum of 80 iterations for the production runs. However, during the execution of the production runs it is advised to check whether the convergence in the area of interest and at the output locations is okay.

There are no measurements available to validate the model. The results look logical and show no abnormalities. Apart from the output locations, the model is suitable for use for BOI production computations.

Samenvatting

Dit rapport beschrijft de modelopzet van swan-hvbb-hr2023_6-v1a, het SWAN-model voor Haringvliet-Biesbosch. Het model is opgezet voor BOI-productieberekeningen. BOI staat voor ‘Beoordelings- en Ontwerp Instrumentarium’.

Het kromlijnige rekenrooster is overgenomen van de vorige modelversie (Deltares, 2016). We hebben de bodemligging en obstakels aangepast. De richtingsresolutie bedraagt 5°. Het model maakt gebruik van SWAN-versie 41.31A.1 en gebruikt de generieke instellingen zoals aanbevolen in Deltares (2021a en 2021b). De wind en waterstand worden uniform over het hele domein verondersteld. Stroming wordt niet meegenomen.

Er zijn zestien testberekeningen uitgevoerd voor de combinaties van hoge en lage windsnelheid (47 m/s en 10 m/s), hoge en lage waterstand (NAP+7 m en NAP-1 m) en vier richtingen (67.5°N, 202.5° N, 270°N, 315°N). De berekeningen hebben geen opvallende zaken aan het licht gebracht. Ons advies is om een maximum van 80 iteraties aan te houden en daarbij te controleren of de convergentie in het interessegebied en op de uitvoerlocaties in orde is.

Er zijn geen metingen beschikbaar om het model te valideren. De resultaten zien er logisch uit en vertonen geen onvolkomenheden. Het model is geschikt om in te zetten voor BOI productieberekeningen.

Contents

1 Introduction

1.1 General

For safety against flooding in the Netherlands, it is important to know the hydraulic loads, e.g. water levels and waves, that are expected on the Dutch flood defenses during extreme events. The BOI project ('Assessment and Design Instrumentation') by Rijkswaterstaat organizes that this information is present and that a legal safety assessment of the flood defences can be done. To determine the waves, use is made of the numerical wave model SWAN. The SWAN computations that are made in this assessment concern many combinations of (often extreme) wind speeds and water levels, the so-called production computations.

The KPP project “MA07ab 2021 – Hydraulische Schematisaties – Zoet en Zout” provides the hydraulic model schematizations for Rijkswaterstaat and therefore also the SWAN model schematization of the Haringvliet-Biesbosch. Where possible, it strives for coherence and consistency, not only between areas and applications, but also between hydrodynamics and waves. A D-HYDRO model has recently been built for the hydrodynamics (Deltares, 2020b).

To be consistent with other domains and to make use of the latest bathymetric data, the existing SWAN model schematization of the Haringvliet-Biesbosch (hvbb) which was called swan-Rijnmaasmonding (swan-rmm; Deltares, 2016) needs an update. We use the name swan-hvbb to distinguish from the dflowfm2d-rmm-domain covering a larger part of Rijn-Maasmonding.

The Haringvliet-Biesbosch domain consists of (from west to east) the Haringvliet - which is a former estuary but since 1970 partly separated from the North Sea by the Haringvlietdam – the wide Hollands Diep and the Biesbosch tidal area with dozens of smaller canals, three fresh water reservoirs and the Noordwaard polder, enclosed between the Nieuwe Merwede in the North and the Amer in the South.

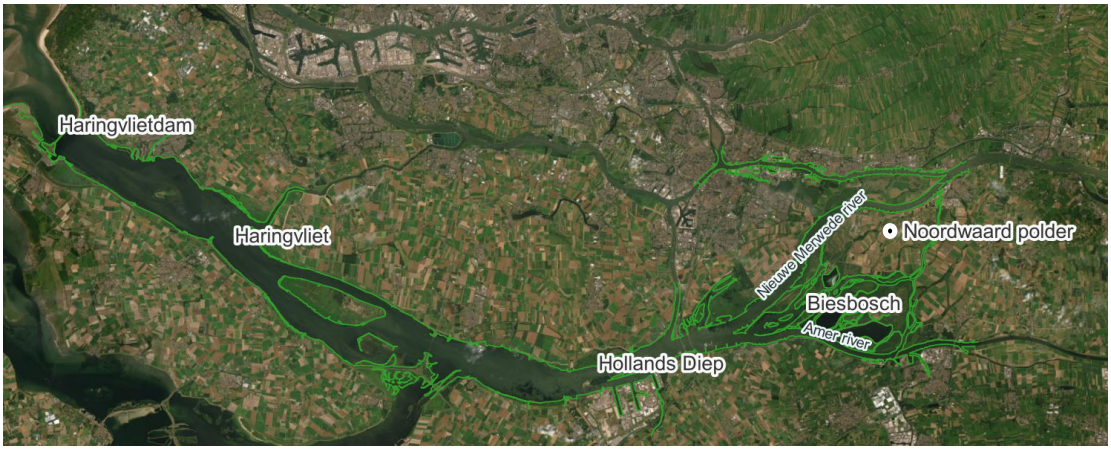

Figure 1.1: Area of interest (green line is land boundary for the area of interest)

1.2 Objective

The aim of this project is to make a SWAN model update for the Haringvliet-Biesbosch area - based on the existing swan-rmm model (Deltares, 2016) - for production computations of waves for BOI. The model will be named swan-hvbb-hr2023_6-v1a.

1.3 Approach

First, the requirements and wishes from BOI were listed and relevant data were examined, such as the data available in Baseline-nl_land and the existing curvilinear computational grid for swan-rmm (Deltares, 2016). For the model settings we followed the advice from Deltares (2021a, 2021b) and Rijkswaterstaat, 2022.

Next, we made the Baseline projections to the SWAN grid and added a few adjustments as suggested in Rijkswaterstaat, 2022, concerning bathymetry and obstacle height, resulting in the new swan-hvbb model.

Subsequently, we performed sixteen test computations to check whether the computation times are manageable, and the results realistic. These test computations concern the extreme wind speeds (10 and 47 m/s) and water levels (-1.0 and 7 m +NAP) for the wind directions 67.5°N, 202.5°N, 270°N, 315°N. We call these the 'cornerstones' of the matrix of wind and water level combinations to be calculated for the production runs.

Furthermore, we did a test computation for a run which was present in the report Deltares (2016) so that a visual comparison could be done to see the effect of the model update.

For BOI2023, new SWAN models have also been made or the Veluwerandmeren (Deltares, 2021d), the Volkerak-Zoommeer (Deltares, 2021e), the Markermeer and Gooi- en Eemmeer (Deltares, 2021f) and the Grevelingen (Deltares, 2021g). Where possible, equal settings are used. The SWAN model for Europoort will follow shortly.

1.4 Set-up of the report

Chapter 2 discusses the basic model set up. Subsequently, Chapter 3 discusses various aspects of the model setup: grid, bathymetry and obstacles, model settings and output. In Chapter 4 the cornerstone-tests are described. An additional run is described in Chapter 5 to make a global comparison with WBI2017 results from Deltares (2016). The conclusions are given in Chapter 6.

2 Data and naming

2.1 Data

We used baseline-rmm_vzm-beno19_6-v1 to derive the bathymetric data and obstacles for SWAN since the proper version to be used (baseline-rmm_vzm-hr2023_6-v1) was not yet available at the beginning of the project. The applied Baseline version is Baseline 6.2 (2020) Version 6.2.0.2247 with ArcGIS 10.5.1. Note that baseline-rmm_vzm-beno19_6-v1 is identical to baseline-rmm_vzm-hr2023_6-v1, except for the BOI-output locations which have been adjusted in the latter one.

For the output locations two clip contours have been made to take the relevant locations from baseline-nl_land-hr2023_6-v1:
A) covering the swan-hvbb domain
B) covering the dflowfm2d-rmm domain

2.2 Naming and folder structure

The model schematization is called swan-hvbb-hr2023_6-v1a. The naming and folder structure that we propose here follows the structure for D-HYDRO as described in the memo Deltares (2021c).

- boundary_conditions	\ wave	\ *. bnd		
	\ meteo	\ *. wnd or *. nc		
	\ flow	\ *.sheet or *. nc		
		\ *.lev or *. nc		
- computations	\ hr	\ hr2023	\ *runid*	*. swn
			\ *runid*	\ results \
- geometry	\ *. grd	(= grid or computation grid)		
	\ *.bot	(= bottom)		
	\ *. fxw	(= fixed weirs or obstacle)		
	\ output_locations	*. xyn		
- general	\			

The model schematization contains an input file (*.swn) in the *computations folder* with an obstacle (*.fxw) and bottom file (*.bot) in the *geometry folder.* The output locations are given in the folder *geometry / output_locations..* The output of the computation ends up in the subfolder *results* in the runid folder within *computations.* The *boundary_conditions, initial_conditions* and *general* folders are not used within this model schematization.

The 'runid ' is the run identifier. In the present study we use the following naming convention: <area>U<wind speed>D<wind direction>Z<plus 'p' or minus 'm'><water level>V<variant>. So, for example run 'hvbbU47D203Zp100Va' has a wind speed of 47 m/s, wind direction of 202.5°N (rounded up to 203°N) and positive water level (‘*Zeewaterstand*’) of 100 cm+NAP. The last letter concerns the variant, to be able to distinguish if any adjustments are made. This name can also be used in the so called ‘sums generator’ (SGWM) to set up a set of runs.

Specifically, for the Haringvliet-Biesbosch, the naming of the model schematization for the above example (hvbbU32D270Zp200Va) has been completed as follows:

- computations	\ hr	\ hr2023	\ U32D270Zp200Va	\ hvbbU32D270Zp200Va.swn
			\ U32D270Zp200Va	\ results \

- geometry \ hvbb-hr2023_6-v1a.grd (=computational grid)
\ hvbb-hr2023_6-v1a.bot (=bottom)
\ hvbb-hr2023_6-v1a.fxw (=fixed weirs or obstacle)
\ output_locations \ swan-hvbb-hr2023_6-v1a_0_all_obs.xyn
\ output_locations \ swan-hvbb-hr2023_6-v1a_4_boi_obs.xyn
\ output_locations \ swan-hvbb-hr2023_6-v1a_5_100m_obs.xyn
\ …

3 Model set-up

3.1 Introduction

The SWAN model for the Haringvliet-Biesbosch has been set up for stationary computations with uniform wind and water levels, according to the advice in Deltares (2020a, 2021a). Because the impact of waves from elsewhere reaching the area is negligible, wave boundary conditions are not used. The waves are generated by the local wind.

This chapter provides an overview of the model set-up. The model design is as consistent as possible with the Veluwerandmeren, Volkerak-Zoommeer, Grevelingen en Markermeer, see Deltares (2021d, 20221e, 2021f, 2021g). An example of a SWAN input file is given in Appendix A.

3.2 Computational grid and bathymetry

The Haringvliet-Biesbosch domain consists of (from west to east) the Haringvliet, the wide Hollands Diep, the Biesbosch tidal area and the Noordwaard polder (see Figure 3.1).

The computational grid is taken exactly from Deltares (2016). It was also used for the WBI2017 production runs. A summary of the number of cells for the curvilinear grid used in the model is found in Table 3.1.

Table 3.1: Computational grid

number of points in x dir	number of points in y dir	total number of grid points	number of active grid points	minimum cell size [m]	maximum cell size [m]
908	3425	3109900	1168922	5	34

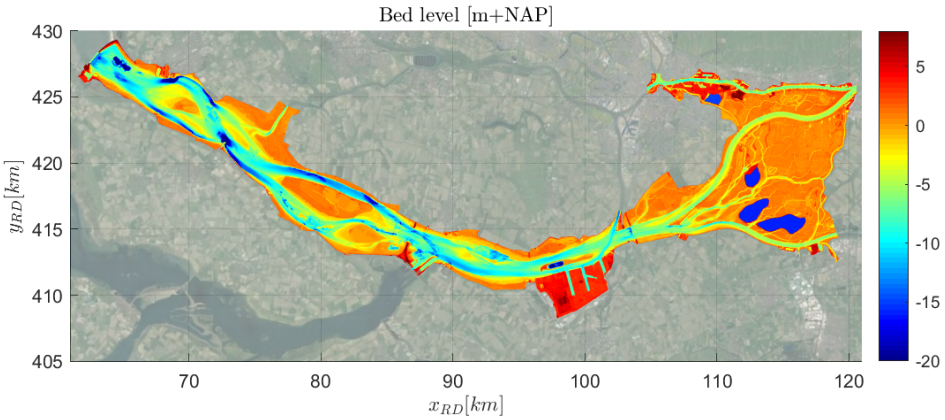

Figure 3.1: Computational domain and bathymetry

Figure 3.2 and Figure 3.3 show details of the computation grid for three areas. The red markers are a selection of the output locations in that specific area.

Figure 3.2: Detailed overview of the computation grid at Heliushaven (left panel) and marina Biesbosch (right panel. The red markers represent output locations.

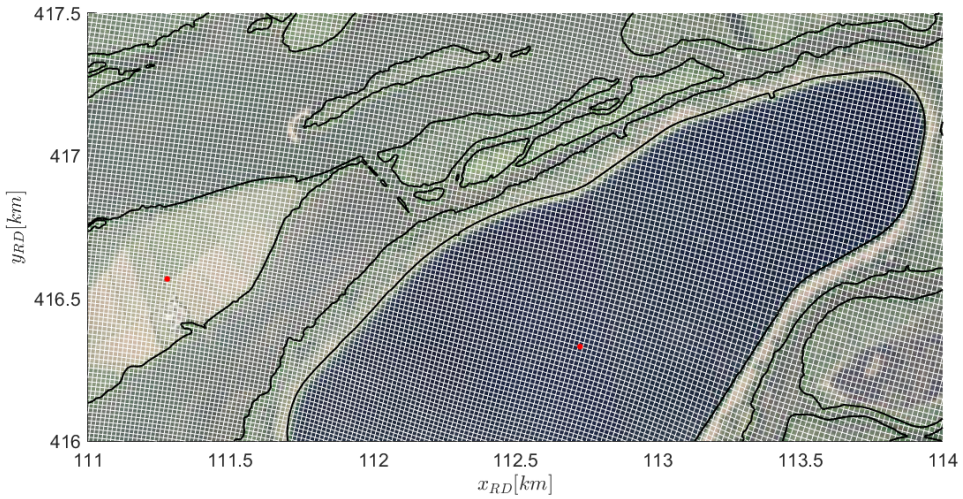

Figure 3.3: Detailed overview of the computation grid for the channels and the reservoir Honderdendertig at the Biesbosch. The red markers represent the provisional output locations.

The Baseline data of baseline-rmm_vzm-beno19_6-v1 was used to construct the bottom of the SWAN model, using Bas2SWAN and the Baseline special (Baseline 6.2 (2020) Version 6.2.0.2247 with ArcGIS 10.5.1). The bathymetry file fits the curvilinear computational SWAN grid but the projection misses three items which were manually adjusted, as advised by Rijkswaterstaat, 2022:

- Small missing parts of Noordwaard near X=118000 Y=420000 has been filled (see Figure 3.4). Data for this was taken from baseline-rmm_vzm-beno19_6-w2.
- Bed level of reservoir ‘Petrusplaat’ adjusted from the original NAP-1.5 m to a uniform NAP-16 m (see Figure 3.5)
- Bed level of reservoir ‘Grote Rug’ adjusted from the original NAP+2.5 m to a uniform NAP-16 m (see Figure 3.6)

The resulting bathymetry file is called hvbb-hr2023_6-v1a.bot.

Note that baseline-rmm_vzm-beno19_6-v1 is identical to baseline-rmm_vzm-hr2023_6-v1 except for the BOI output locations which are only present in the latter one.

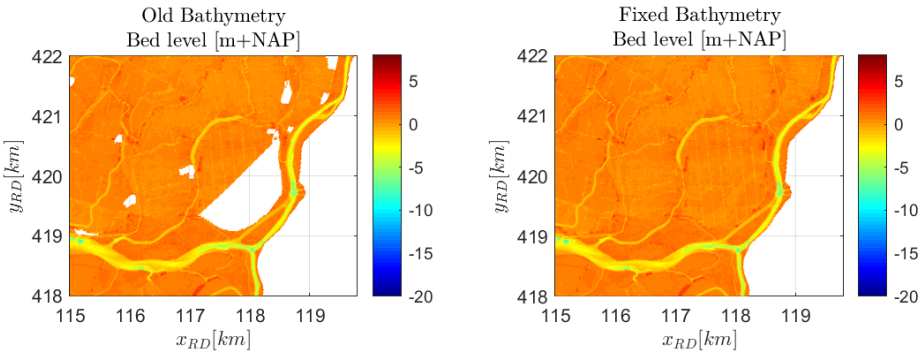

Figure 3.4: Adjustment of the missing bed in the area of the Biesbosch (Noordwaard)

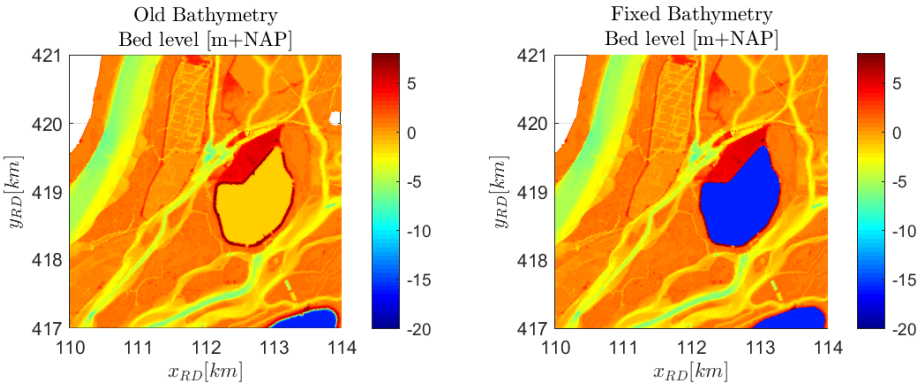

Figure 3.5: Adjustment of the bed level of the reservoir Petrusplaat at the Biesbosch

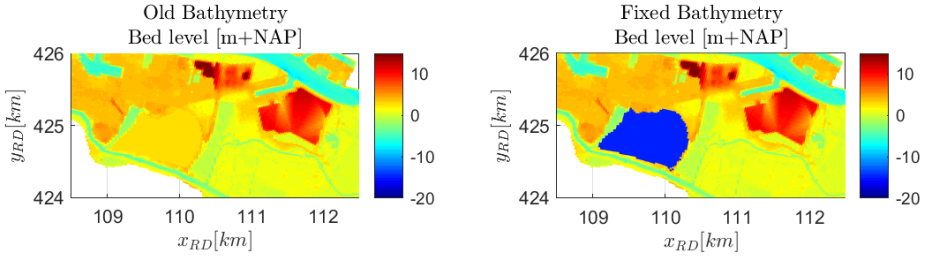

Figure 3.6: Adjustment of the bed level of the reservoir Grote Rug near Dordrecht

In the bathymetry file that comes from Bas2SWAN, the positive values are above NAP. SWAN, on the other hand, expects the positive values to point downwards. In the SWAN input file it must therefore be indicated that the bottom values must be multiplied by -1.

Figure 3.1 shows the bed level of the model schematization of the Haringvliet-Biesbosch domain, after the manual adjustments.

3.3 Obstacles

Most of the dams and breakwaters in the area are too small to capture in the model bathymetry for the present model resolution. Those dams and steep foreshores are therefore described with sub-grid elements (obstacles; also called fixed weirs).

The obstacle file is derived from the Baseline branch baseline-rmm_vzm-beno19_6-v1. With BAS2SWAN, the obstacle file (hvbb-hr2023_6-v1a.fxw) containing the location and height of the obstacles was created for the computational grid.

Manually, we made the following adjustment, as advised in Rijkswaterstaat (2022)

- The height of the obstacles surrounding the reservoirs at Biesbosch has been set at NAP+9m (see Figure 3.8)

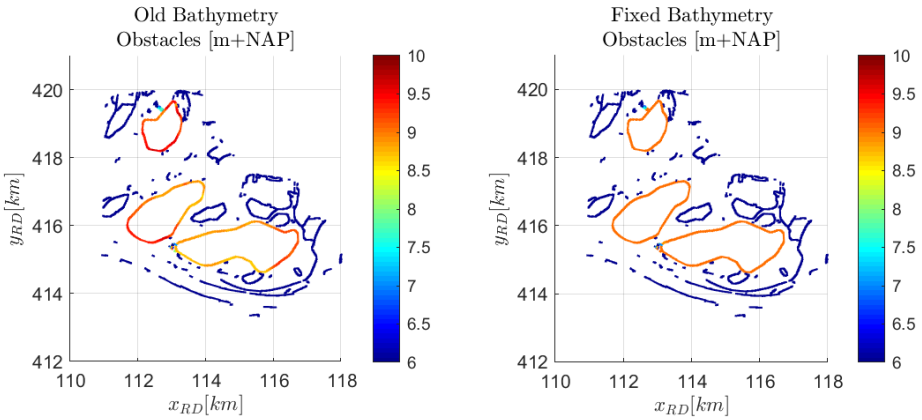

Figure 3.7: Adjustment of the obstacles surrounding the reservoirs at Biesbosch

All obstacles are defined as dams according to the Goda formulation with default values (α =2.16 and β=0.15) for determining the transmission coefficients that depend on the incoming wave and the obstacle height. Wave reflection is not taken into account (reflection=0). Note that the processes that occur near these small-scale obstacles are in principle not solved by SWAN (reflection and diffraction), but by adding the obstacles the influence of these small-scale geometries on the wave energy is simplified and schematized by empirical relations.
The obstacles are presented to the SWAN input file (*.swn) in a separate file via the INCLUDE option. Figure 3.8 gives an overview of the position and height of the obstacles.

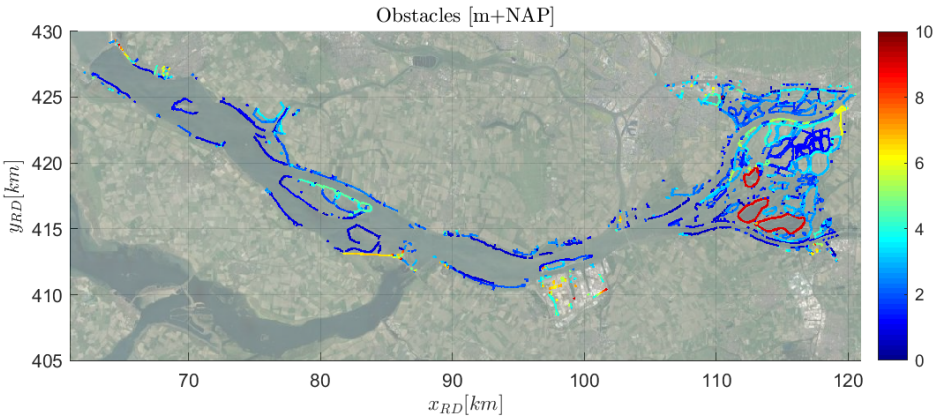

Figure 3.8: Location of obstacles with height in colour

To illustrate the effect of the obstacles, the wave height and wave direction are shown for two example areas with obstacles and a complex bottom. Figure 3.9 shows a detailed view of the Tiengemeten island. The breakwaters, surrounding the south of the island and located at the left bank of the Haringvliet, are represented by obstacles with heights below 2 m. Additionally,

the roads on top of the dikes are defined as obstacles with varying heights. It is noted that for a water level of NAP+2 m, the obstacles located in the northeast of the island block the waves.

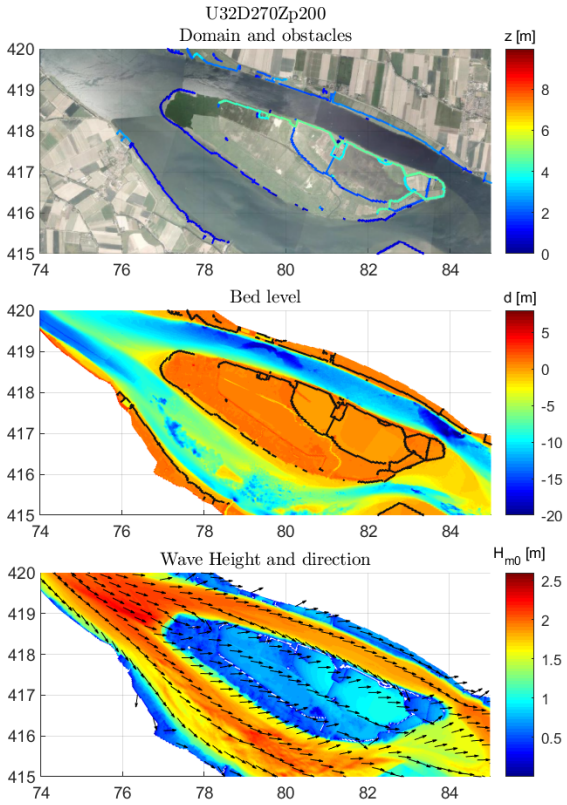

Figure 3.9: Domain with obstacles (upper panel), bottom with obstacles (middle panel) and wave height with wave direction (lower panel) for the Tiengemeten island. The computation concerns a wind speed of 31.7 m/s, a water level of NAP+2 m and a wind direction of 270°N.

In Figure 3.10, part of the Biesbosch is displayed. For this area, the borders of the reservoirs are represented by obstacles with a height of NAP+9 m.

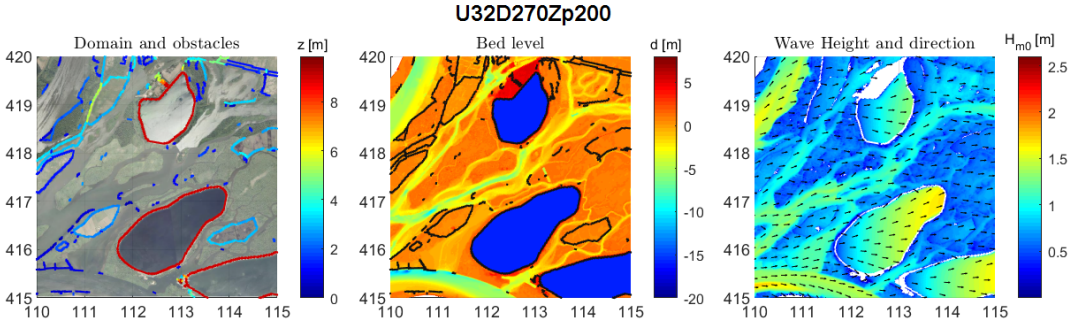

Figure 3.10: Domain with obstacles (left panel), bottom with obstacles (middle panel) and wave height with wave direction (right panel) for the Biesbosch area. The computation concerns a wind speed of 31.7 m/s, a water level of NAP+2 m and a wind direction of 270°N.

3.4 Spectral space

The spectral space is defined by wave frequencies and wave directions. Concerning the directions, the full circle is considered so that waves can travel in any direction. The 360° have been discretized by 72 bins each 5° wide.

The frequency domain stretches from 0.06 to 2.4 Hz and is logarithmically divided in 39 bins, conform Deltares (2020a) and Rijkswaterstaat (2022). This means that waves with periods between 0.4 and 16 s are considered, which is wide enough for this area.

3.5 Wind and water levels

The model uses uniform wind and water levels whose values are specified in the SWAN input file. SWAN interprets the imposed wind speed as the local wind at a height of 10 m (U10). It is up to the user to convert any other wind input (potential wind, wind shear stress, ...) to U10. If one wants to use a wind drag other than that available in SWAN, this can be solved via a so-called pseudo wind (see Deltares, 2020a). Elaboration on the pseudo wind is not part of the current model set-up.

The wind drag formulation according to Wu (1982) is applied, capped at Cd=0.00275 see Deltares (2021a) and 3.6.1.

No currents are used in the model schematization. This is in accordance with the advice of Deltares (2021a). Because no significant waves from elsewhere can reach the Haringvliet-Biesbosch domain, wave boundary conditions are not present.

If a user wishes, the SWAN_input file can be adapted so that spatially varying wind and/or water level fields can be applied.

3.6 Model settings

3.6.1 Physics

For the physical settings, we follow the recommendations as described in Deltares (2020a, 2021a and 2021b). This means that the Westhuysen formulations are used for wind generation, white capping and shallow water breaking. These were also used for WTI2011 and WBI2017 computations. Differences compared to WBI2017 concern the wind drag capping of the Wu formulation. The physical settings are specified in the SWAN input file as follows:

```
GEN3 WESTH
WCAP WESTH   cds2=5.0e-05 br =0.00175 p0=4.0 powst =0.0 powk =0.0 &
              nldisp =0.0 cds3=0.8 powfsh =1.0
QUAD         iquad =2 lambda=0.25 Csh1=5.5 Csh3=-1.25
BREA WESTH   alpha=0.96 pown =2.5 bref =-1.39630 shfac =500.0
FRICTION     JONSWAP CFJON 0.038
TRIAD        itriad =11 trfac =0.1 cutfr =2.5
```

- For wind generation and white capping, the formulation of Van der Westhuysen et al. (2007). This is different from the default SWAN settings for version 41.31A.1;
- The default settings for quadruplets;
- For depth-induced wave breaking, the formulation of Van der Westhuysen (2010). This is different from the default SWAN settings for version 41.31A.1.
- For bottom friction the default value Cf=0.038 m^2/s^3;
- For triads the triad formulation is LTA-OCA (‘Lumped Triad Approximation’ – ‘Original Collinear Approximation’), by Eldeberky (1996). This is indicated with itriad =11. As proportionality coefficient we use trfac = 0.1.

In addition, we use:

- Wu's drag relationship (1982). This is not default in version 41.31A.1.
- Wind drag cut-off at Cd=0.00275, this corresponds to a wind speed of 30 m/s. This is not default in version 41.31A.1.
- Water density 1000 kg/m^3

3.6.2 Numerics

For the numerical settings we use the recommendations as described in Deltares (2021a), but without the dabs =0.0 shown therein erroneously.

```
NUM STOPC dabs=0.005 drel =0.01 curvat =0.001 npnts =101. STAT mxitst =80 alpha=0.001
```

The model is forced to calculate 80 iterations each run. It is recommended to check convergence using test output, see also Section 4.3.

3.7 Output Locations

The output locations for the BOI production runs are defined in seven files:

swan-hvbb-hr2023_6-v1a_0_all_obs.xyn	
swan-hvbb-hr2023_6-v1a_1_kilometer_obs.xyn	(thalweg locations every 1 km)
swan-hvbb-hr2023_6-v1a_2_output_obs.xyn	
swan-hvbb-hr2023_6-v1a_3_measurement_obs.xyn	
swan-hvbb-hr2023_6-v1a_4_all_boi_obs.xyn	(derived for hr2023)
swan-hvbb-hr2023_6-v1a_5_100m_obs.xyn	(thalweg locations every 100 m)
swan-hvbb-hr2023_6-v1a_6_20m_obs.xyn	(thalweg locations every 20 m)

These files were made via a Baseline projection with Bas2WAQ on the SWAN grid (Bas2SWAN does not provide output locations) and contain only locations within the swan-hvbb domain. Note that there are also larger files available for the entire dflowfm2d-rmm-domain (rmm is the abbreviation for Rijn-Meuse-mouth). The SWAN locations are a subset of those DFLOW-FM locations. It is up to the user which set of output locations to use. The disadvantage of those larger files is that many locations will have no wave results since they lie outside the swan-hvbb domain. The advantage is that they are also used in dflowfm2d so that the wave results and hydrodynamic results can easily be combined. These are called as follows:

rmm-vzm-hr2023_6-v1a_0_all_obs_obs.xyn	
rmm-vzm-hr2023_6-v1a_1_kilometer_obs.xyn	(thalweg locations every 1 km)
rmm-vzm-hr2023_6-v1a_2_output_obs.xyn	
rmm-vzm-hr2023_6-v1a_3_measurement_obs.xyn	
rmm-vzm-hr2023_6-v1a_4_all_boi_obs.xyn	(derived for hr2023)
rmm-vzm-hr2023_6-v1a_5_100m_obs.xyn	(thalweg locations every 100 m)
rmm-vzm-hr2023_6-v1a_6_20m_obs.xyn	(thalweg locations every 20 m)

Figure 3.11 shows the 6497 locations of swan-hvbb-hr2023_6-v1a_4_all_boi_obs.xyn. From this set, eight locations have been selected to present the spectral output.

Note that there are duplications in these sets. To prevent duplications, do not include in the *.swn file:
*hr2023_6-v1a_0_all_obs_obs.xyn
*hr2023_6-v1a_1_kilometer_obs.xyn
*hr2023_6-v1a_6_20m_obs.xyn

The file *hr2023_6-v1a_4_all_boi_obs.xyn contains the basis HR locations, fall back locations and extra locations.

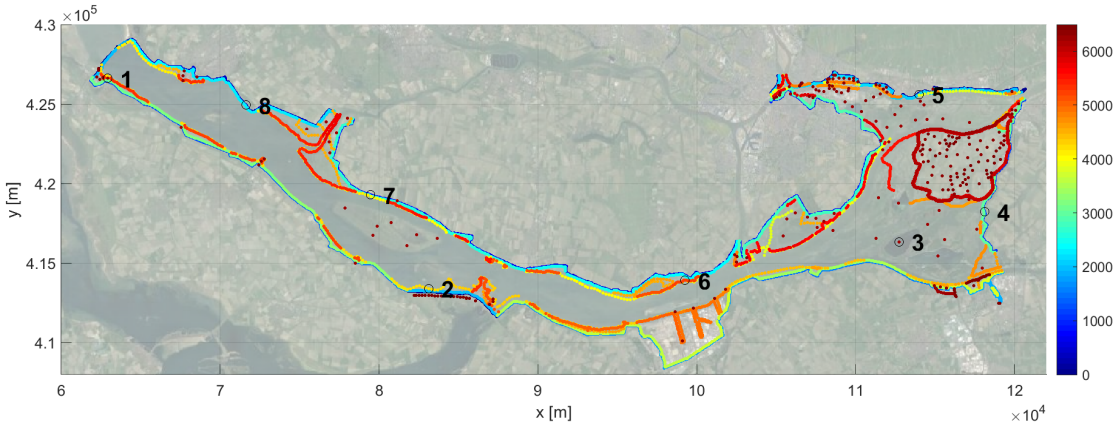

Figure 3.11: Output locations (swan-hvbb-hr2023_6-v1a_4_all_boi_obs.xyn) with location number in color; numbered black circles indicate output locations for spectra

3.8 SWAN version

The most recent SWAN version available from Deltares is used. At the time of the study, this was SWAN version 41.31A.1. This is a Deltares version and, unlike the official TU-Delft version, it does contain the settings used for WBI2017 settings (such as the Van der Westhuysen formulation for breaking).

4 Corner stone analysis for BOI

4.1 Method

To check whether the SWAN model for the Haringvliet-Biesbosch can be applied for BOI production computations, we perform some test computations focusing on computation times, convergence, stability and whether the results are realistic.

For these test computations, we choose the extreme wind speeds and water levels (the so-called 'corner stones') for a number of relevant wind directions from the matrix of wind and water level combinations to be calculated for the production computations. The variations were determined on the basis of the stochastic report (Stijnen et al., 2021). Note that these corner stones are not necessarily realistic conditions, but they are important for filling the matrix of conditions. It is therefore important that the SWAN model can also be applied to these (unrealistic) corner stones. It is expected that if the model does not encounter any problems in stability and convergence behavior for those conditions, there will probably be no problems for the intermediate combinations.

Table 4.1: variations for the corner stone analysis

	runid	Wind speed [m/s]	Wind direction [°N]	Water level [m+NAP]
1	**U10D068Zm100**	10	67.5	-1.0
2	**U10D068Zp700**	10	67.5	7.0
3	**U10D203Zm100**	10	202.5	-1.0
4	**U10D203Zp700**	10	202.5	7.0
5	**U10D270Zm100**	10	270	-1.0
6	**U10D270Zp700**	10	270	7.0
7	**U10D315Zm100**	10	315	-1.0
8	**U10D315Zp700**	10	315	7.0
9	**U47D068Zm100**	47	67.5	-1.0
10	**U47D068Zp700**	47	67.5	7.0
11	**U47D203Zm100**	47	202.5	-1.0
12	**U47D203Zp700**	47	202.5	7.0
13	**U47D270Zm100**	47	270	-1.0
14	**U47D270Zp700**	47	270	7.0
15	**U47D315Zm100**	47	315	-1.0
16	**U47D315Zp700**	47	315	7.0

From the sixteen directions (from 22.5° with steps of 22.5° to 360°) we selected 67.5°N, 202.5°N, 270°N and 315°N. Given the shape of the area of study (northwest to southeast and then to northeast), the chosen directions present both large and small fetches depending on the location along the domain.

For the corner stone analysis, we apply the wind speeds as if it were the open water wind U10, but in the production computations it may be potential wind and a conversion to U10 would have to be made.

We consider not only the results at the output locations but also the overall image from spatial map output of the computed wave parameters.

4.2 Results

4.2.1 Map output

An overview has been made for all sixteen computations of six parameters, namely the bed level, wave height (H_{m0}), wave period ($T_{m-1.0}$), the wave direction in relation to the wind direction (this gives an idea where a lot of refraction occurs) and dHs and dTm. These last two parameters give the difference in wave height and wave period T_{m01} between the last and penultimate iteration, respectively. This is an indication for the convergence.

As an example, Figure 4.1 shows the result of computation U47D068Zp700 (47m/s wind from 67.5°N, water level 7m+NAP). The spatial results show no abnormalities. The wave height increases to 4 m at the west side and the period to around 5 s.

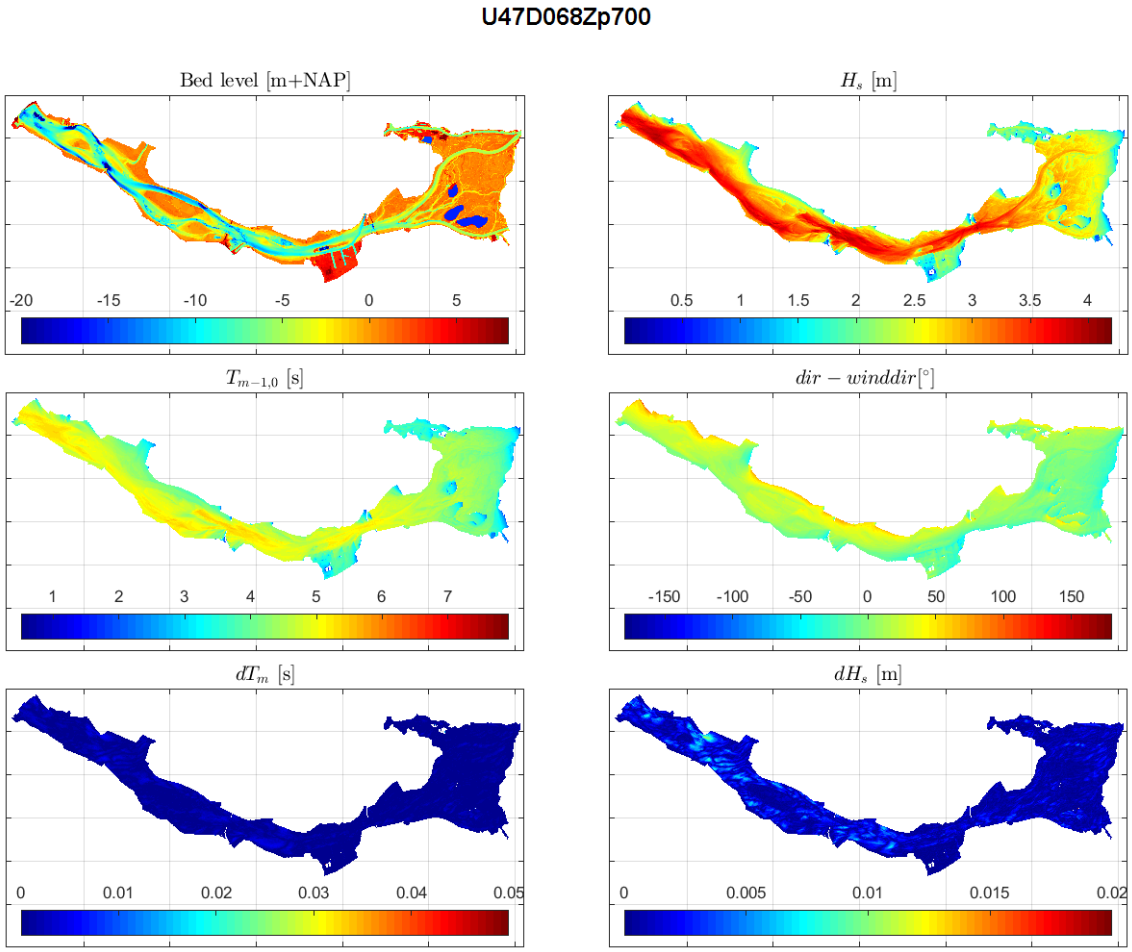

Figure 4.1: Results U47D068Zp700 (47m/s wind from 67.5°N, water level 7m+NAP)

For water levels of NAP+7 m and wind speeds of 47 m/s, the waves at much of the Haringvliet are usually larger than 3.0 m, regardless of the wind direction. For the same conditions in the Biesbosch region, the waves are generally below 3 m, except for the wind direction of 203 °N,

when the long fetches cause higher waves. In run U47D068Zp700 (see Figure 4.1), waves higher than 3 m are also present at the Hollands Diep, whilst the smallest waves are computed in the eastern part of the Biesbosch. Note that this extreme high water level covers almost the entire Biesbosch with water.

The panels with convergence parameters (dTm and dHs) show no extreme outliers and the change in the last iteration, for this corner stone simulation is less than 0.12 s and 0.01 m. For the vast majority of the grid points the value of dHs is less than 0.005 m.

The computation in Figure 4.1 was also performed for a low water level of NAP-1 m. The main difference between this case (see Figure 4.2) and the previous one is the amount of dry land along the entire domain, mainly at the banks of the Haringvliet and Hollands Diep and the Biesbosch region. Furthermore, these low water levels result in much lower waves due to breaking and bottom friction and possibly also due to shorter fetches

For the sixteen corner stone computations the results look realistic. It should be noted that not all plots are included in the report. The maximum wave heights occur at locations with relatively large fetch lengths and relatively large water depths. In the region close to Dordrecht, north of the Nieuwe Merwede, the wave heights are less high, but can increase above 2.5 m for a high water level, a very extreme wind speed of 47 m/s and a wind direction with large fetch.

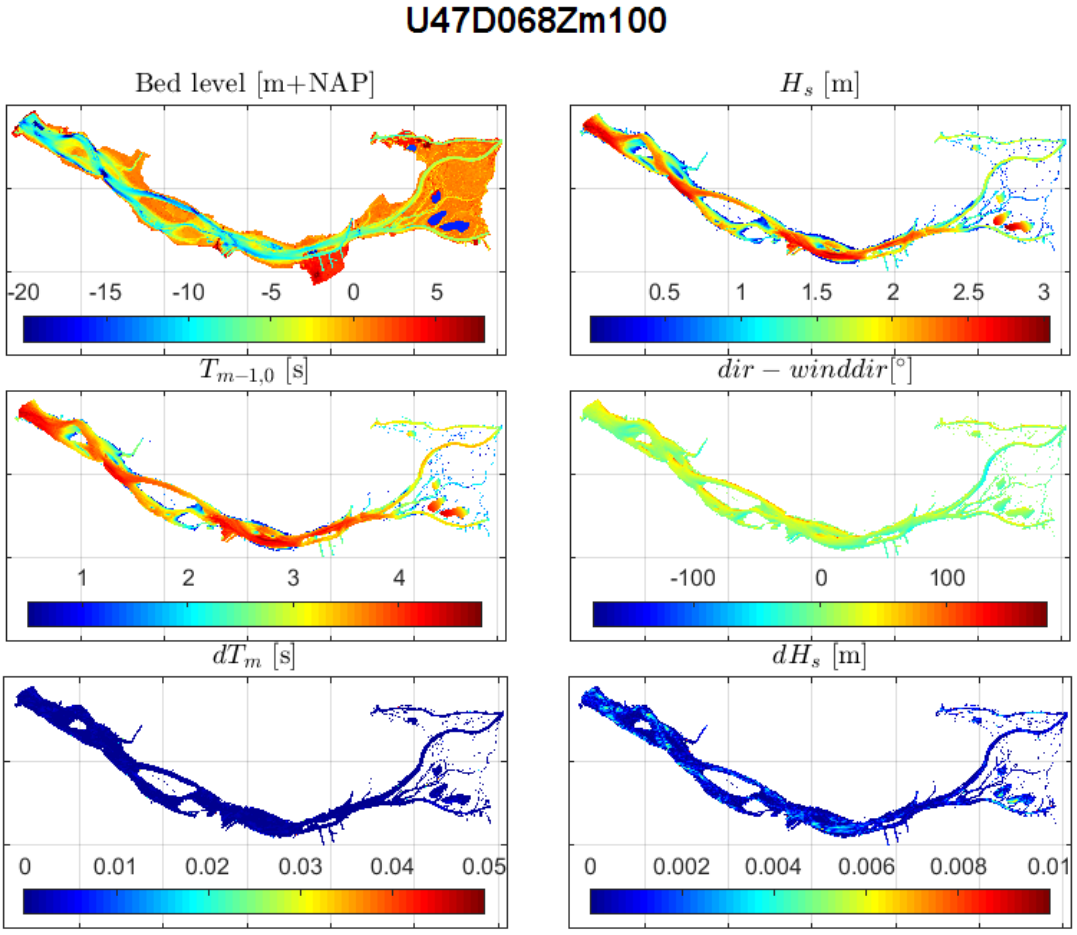

Figure 4.2: Results U47D068Zm100 (47m/s wind from 67.5°N, water level -1m+NAP)

4.2.2 Map output, wave steepness and Ursell number

Besides the standard wave parameters, also two derived wave parameters are considered to verify the model results: the deep water wave steepness S and the ursell number U_r.

The deep water wave steepness is defined as wave height over wave length: $H/L_{m-1,0}$ with $L_{m-1,0} = \frac{g}{2\pi} T_{m-1,0}^2$.

The Ursell number is a measure for non-linear behavior of the waves, and for the expected role of triads. A high value of the Ursell number indicates non-linear waves and stronger triad interactions. It is given by:

$$U_r = \frac{g}{8\sqrt{2}\pi^2} H_s T_{m01}^2 / d^2$$

With *g* the gravity acceleration, H_s the significant wave height, T_{m01} the mean absolute wave period and *d* the total water depth (taken from the SWAN manual).

For all sixteen cornerstone runs the wave steepness and Ursell number plots are included in Appendix B (Figure B3-B18). The first eight plots concern the low wind velocity of 10 m/s cases, and wave steepness and Ursell number are relatively small. The wind velocity of the final eight plots is 47 m/s and here we see much larger values of wave steepness and Ursell number.
The wave steepness is high when the fetches are short and the wind velocity high (hence young waves), see for instance the southern banks in Figure B-13 (U47D203Zm100). Also, on the northern bank we see relatively steep waves, this could be due to wave shoaling.

The Ursell number depends strongly on water depth. The relatively higher Ursell numbers (circa 0.3) occur in shallow areas, where waves tend to break. In deeper parts, the Ursell number is small. This implies that triads occur locally where the water is shallow.

4.2.3 Map output, detail near transition Hollands Diep Biesbosch

In addition, we analysed the wave height at the transition from Hollands Diep to the Biesbosch region and the effect of the wind direction on the wave field. Figure 4.3 below shows the wave height and direction as well as the bed position and the obstacles for the highest wind speed (47 m/s) and the highest and lowest water level (NAP+7 m and NAP-1 m) for the four different wind directions.

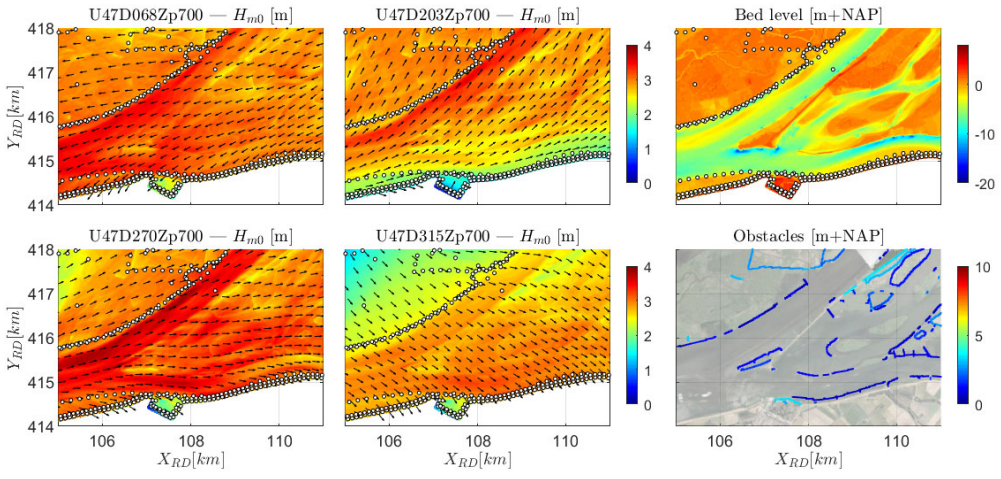

Figure 4.3: Results wave height and wave direction at the intersection of Hollands Diep and Biesbosch at four different wind directions (47 m/s and NAP+7 m). The circles represent the output locations

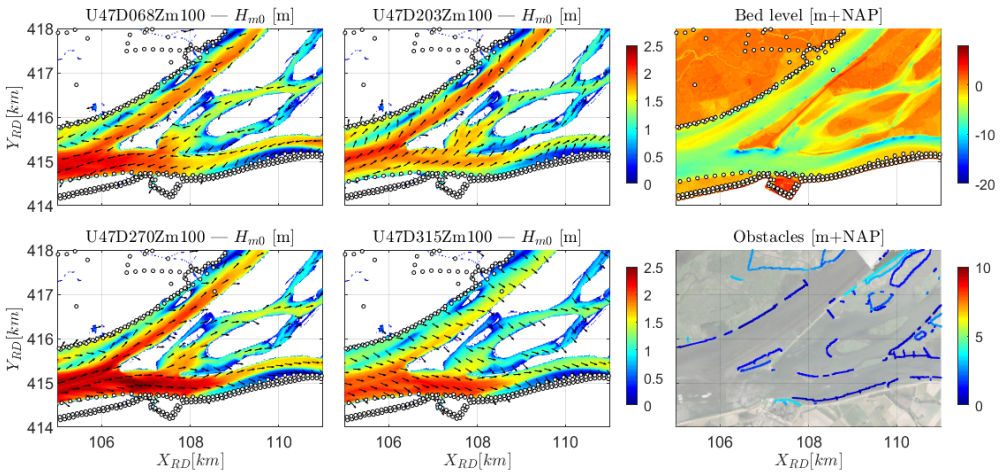

Figure 4.4: Results wave height and wave direction at the intersection of Hollands Diep and Biesbosch at four different wind directions (47 m/s and NAP-1 m). The circles represent the output locations

The waves computed with high water level conditions are high, especially in the main channels above 3 m. The obstacles have little effect on the wave development in this region because the water depth is much larger than the height of the obstacles. On the other hand, for the low water level of -1 m+NAP, there is only water at the channels, thus the shallower areas remain dry. The variation in wave direction is mainly caused by refraction on the shoals located along the main channels.

4.2.4 Results at the output locations

Figure 4.6 shows for a large subset of output locations (see Figure 4.5) the significant wave height and wave period for four different combinations of the highest and lowest wind speed and highest and lowest water levels, all with a wind direction of 67.5°N (D068). On average, the locations are 100-150 m from the crest of the dike. Figure 4.7 presents the calculated wave height and wave period for a wind direction of 202.5°N. The results for the other wind directions are shown at the back of the report in Appendix B (B-19 and B-20).

These plots offer a quick check, like the minimum and maximum values, no extreme outliers, higher wind results in higher waves, the same holds for higher water levels. The maximum values of the significant wave height and spectral wave period $T_{m-1,0}$ (approximately 4 m and slightly above 5 s, respectively) are as expected. It can also be seen that an increase in wind speed leads to an increase in wave height and spectral period for all locations. The same applies to the water level, where a higher water level results in higher and longer waves. It is also visible that during the low water level conditions many locations are dry, so they have no output data. The bottom panel shows the bed level. Especially for low water cases, one can see that locations with larger water depth have higher waves.

The effect of the wind direction cannot be directly related to an increase or decrease in wave parameters due to the shape of the domain of analysis. Depending on the location and the fetch, the wave height and spectral period decrease or increase. For instance, at output locations 600-700 on the north bank of the Haringvliet, the westerly winds return the largest waves due to a combination of wind direction, bed level and available fetch. When the wind direction is ENE (67.5 °N), much smaller waves are resolved by the model given the small fetch.

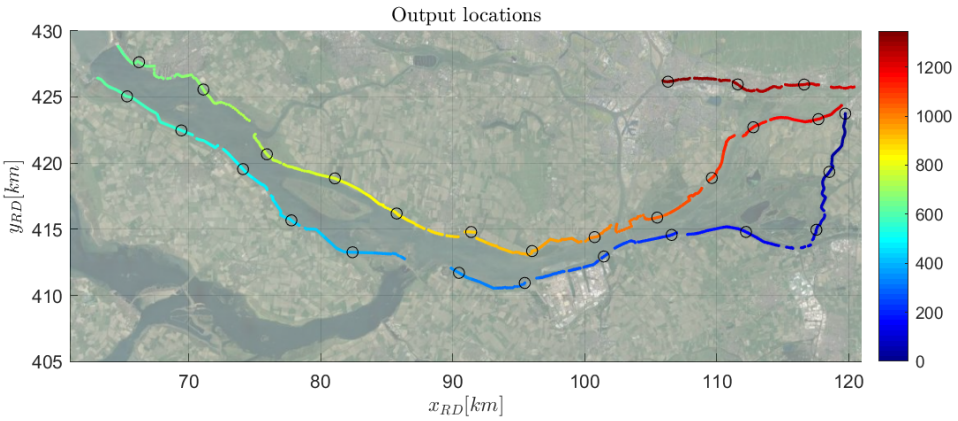

Figure 4.5: Selected output locations with location number in color; circles indicate output locations every 50th point

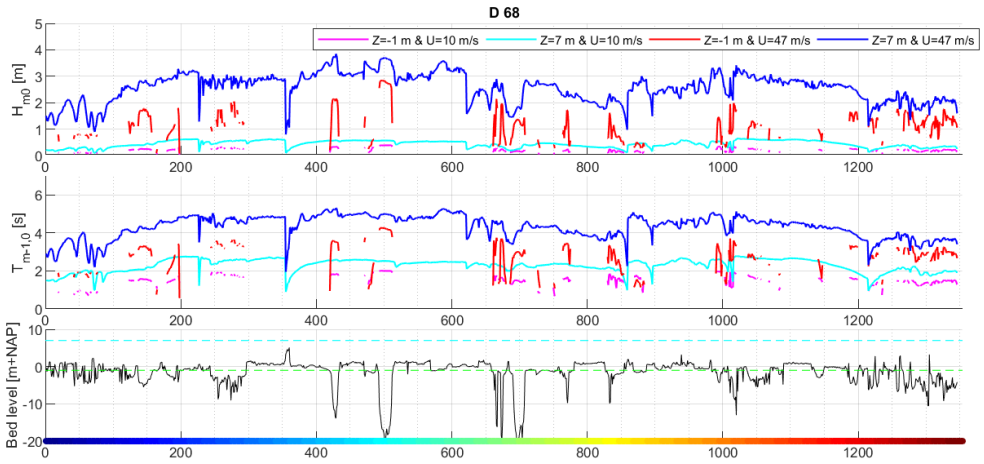

Figure 4.6: SWAN results of wave height (upper panel), wave period (middle panel) and bed level (lower panel) at the output points for four runs with a wind direction of 67.5°N. The color band in the lower panel matches the locations shown in Figure 4.5. The green dotted line represents NAP-1 m and the cyan dotted line indicates NAP+7 m.

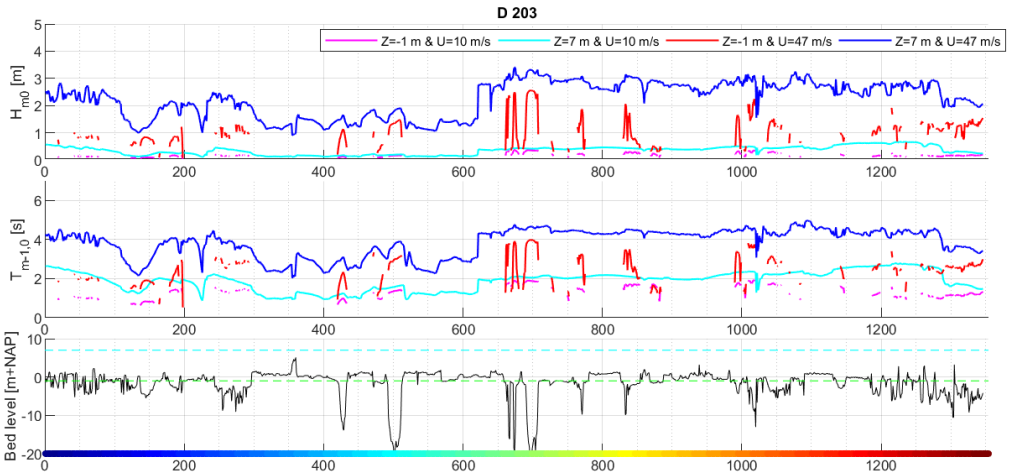

Figure 4.7: SWAN results of wave height (upper panel), wave period (middle panel) and bed level (lower panel) at the output points for four runs with a wind direction of 202.5°N. The color band in the lower panel matches the locations shown in Figure 4.5. The green dotted line represents NAP-1 m and the cyan dotted line indicates NAP+7 m.

4.2.5 Spectra

The wave spectra tell how the wave energy is distributed over the frequencies. The figures below - Figure 4.8 and Figure 4.9 - show the wave spectra for location 8 (see location on map in Figure 3.11) for a low wind speed (top panels; 10 m/s) and high wind speed (second row of panels; 47 m/s) for the two water levels (NAP-1 m and NAP+7 m) and four different wind directions (67.5°N, 202.5°N, 270°N and 315°N). This is mainly to check whether the frequency domain from 0.06 to 2.4 Hz is wide enough and whether the spectra look logical. This has also been checked for other locations, but the figures are not included in this report.

The plots indicate that for wave frequencies above the peak frequency (the right flank), the spectra for a water level of NAP-1m and NAP+7 m are alike. For lower wave frequencies the effect of water level is clearly visible and the runs with NAP+7 m water level result in higher and longer waves.
The wind direction of 67.5°N produces double peaked spectra at the considered location, especially with low water levels. As the wind comes from the land here the waves are a combination of small locally generated waves and waves from the channel coming from the south east. Note that on this location the spectra for this wind direction are far less energetic than for the other wind directions.

Based on the spectra plots, one could consider limiting the maximum frequency, but for consistency and in locations with short fetch lengths where local wind growth is important, it is still recommended that the maximum frequency be 2.4 Hz.

Figure 4.9 shows the same information but on a log scale. The high-frequency flank runs approximately according to f^{-4} as can be expected with Van der Westhuysen's wind growth formulation, see also Deltares (2021a).

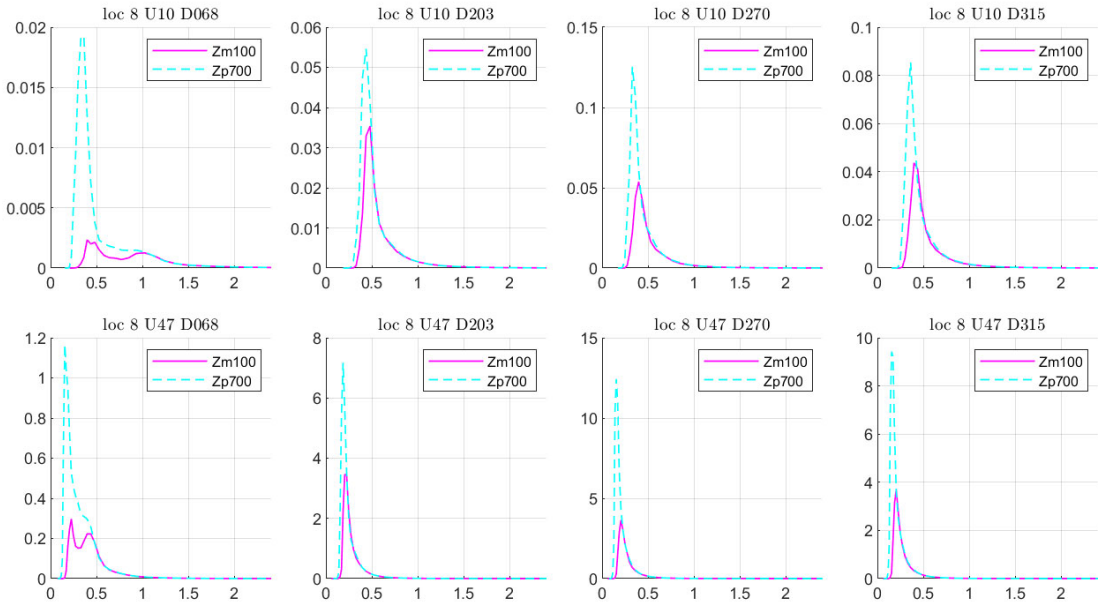

Figure 4.8: Variance density spectra [m^2/Hz] at location 8 (see location on map in Figure 3.11) of the sixteen corner stone computations; the maximum frequency is 2.4 Hz. NB: The y-scales vary

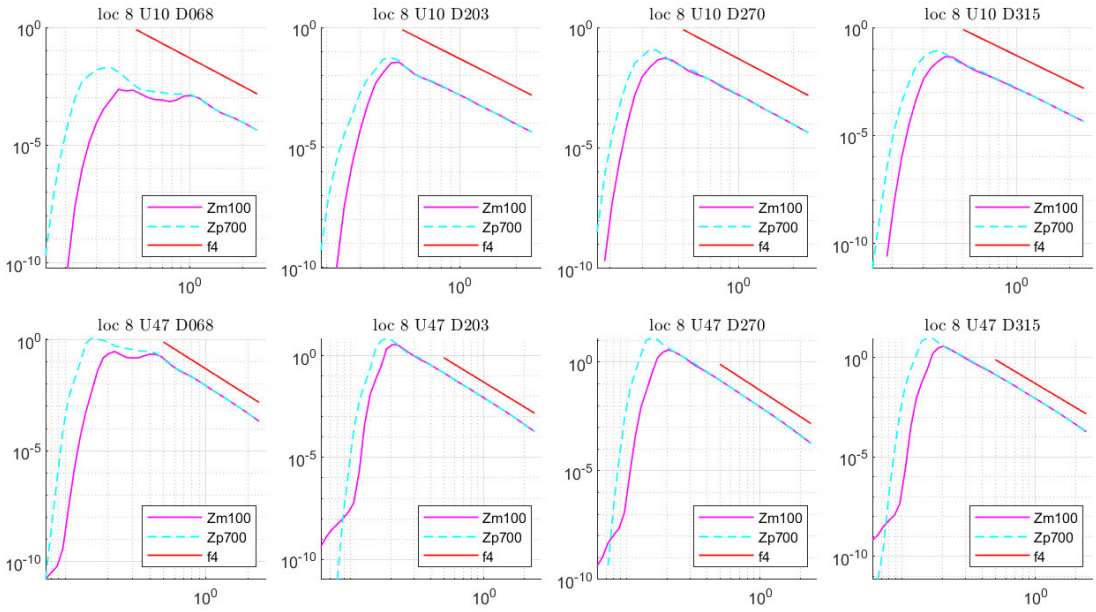

Figure 4.9: Spectra [m^2/Hz] on log scale at location 8 (see location on map in Figure 3.11) of the sixteen corner computations; An f^{-4} tail is plotted with the red line.

4.3 Convergence and computation times

Seven locations have been selected (see Figure 4.10) to verify the convergence behavior of the model based on the wave height H_{m0}, wave period T_{m01}, wave direction and directional spread as a function of the iteration. Note that the standard SWAN output parameters for the convergence behaviour are H_{m0} and T_{m01} whereas we mainly consider the spectral wave period $T_{m-1,0}$ in this report.

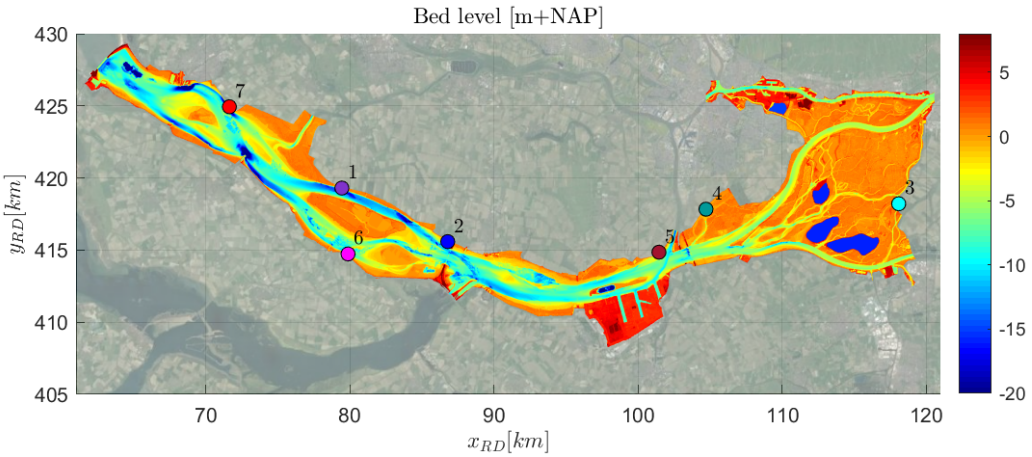

Figure 4.10: Locations of the output points for which the convergence behavior has been analysed. The output points are shown as colored markers.

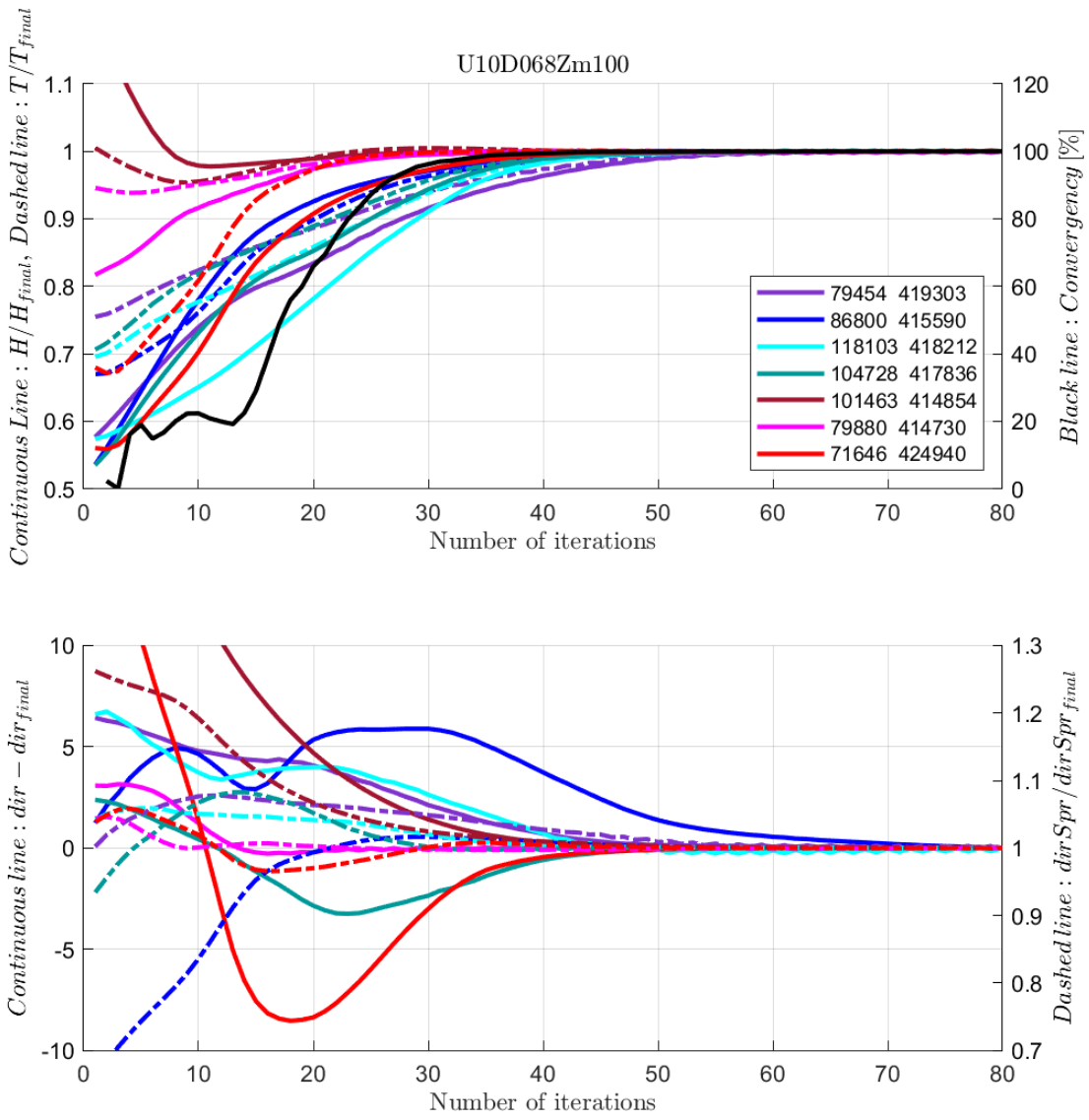

Figure 4.11: Convergence behaviour for U10D068Zm100 for the significant wave height (continuous line, top panel), spectral wave period T_{m01} (dashed line, top panel), percent converged grid points (black line, top panel), direction (continuous line, bottom panel) and directional spread (dashed line, bottom panel). The colors of the locations match the locations in Figure 4.10.

Figure 4.11 shows typical convergence behavior. All computations go through 80 iterations even though most have converged after 60 iterations. The wave height and wave period converge faster than the wave direction and directional spread. In this example, the solution reaches a convergence level of 99.96% of wet grid points. Not all computations converge so well. For instance, Figure 4.12 displays the results for the combination of high wind speed and low water level (U47D203Zm100). Here the percentage of converged grid points after 80 iterations is less (98.94%). Moreover, it is noted that the wave period and the wave direction for the marine blue location (nr 2) (see locations in Figure 4.10) do not converge after 80 iterations. It turns out that for the applied water level of NAP-1 m, this location is close to the water boundary. This makes the location less suitable to check model convergence. As an extra check, Figure 4.13 shows additional plots of dHs, bed level and wave height near the difficult position of location nr 2. The overall convergence of this run looks good.

Also, in Rijkswaterstaat (2022), it is mentioned that the convergence is less for lower water levels and that increasing the number of iterations does not fully solve the problem. Rijkswaterstaat (2022) recommends keeping the maximum number of iterations at 80.

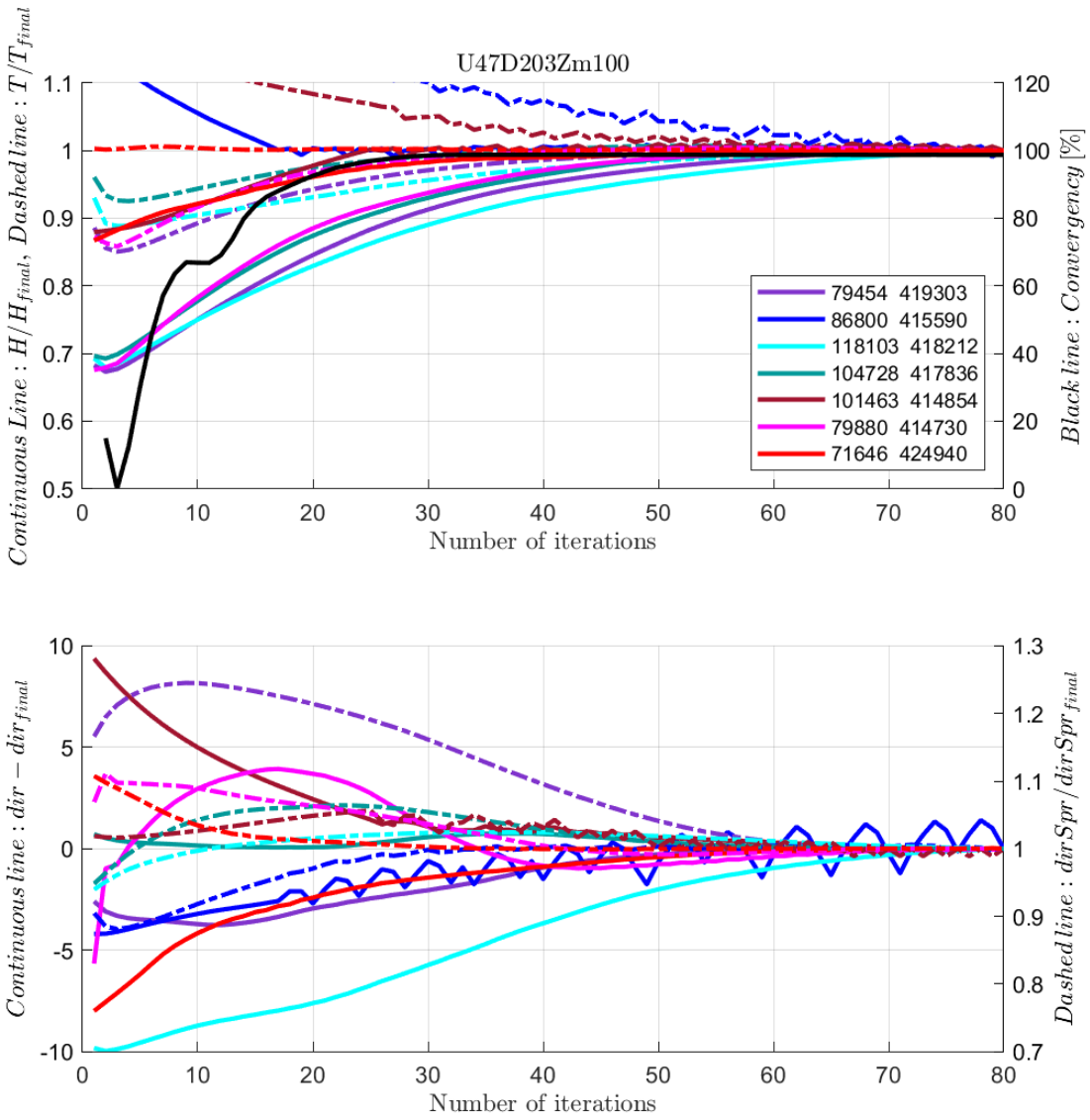

Figure 4.12: Convergence behaviour for U47D203Zm100 for the significant wave height (continuous line, top panel), spectral wave period T_{m01} (dashed line, top panel), percent converged grid points (black line, top panel), direction (continuous line, bottom panel) and directional spread (dashed line, bottom panel). The colors of the locations match the locations in Figure 4.10.

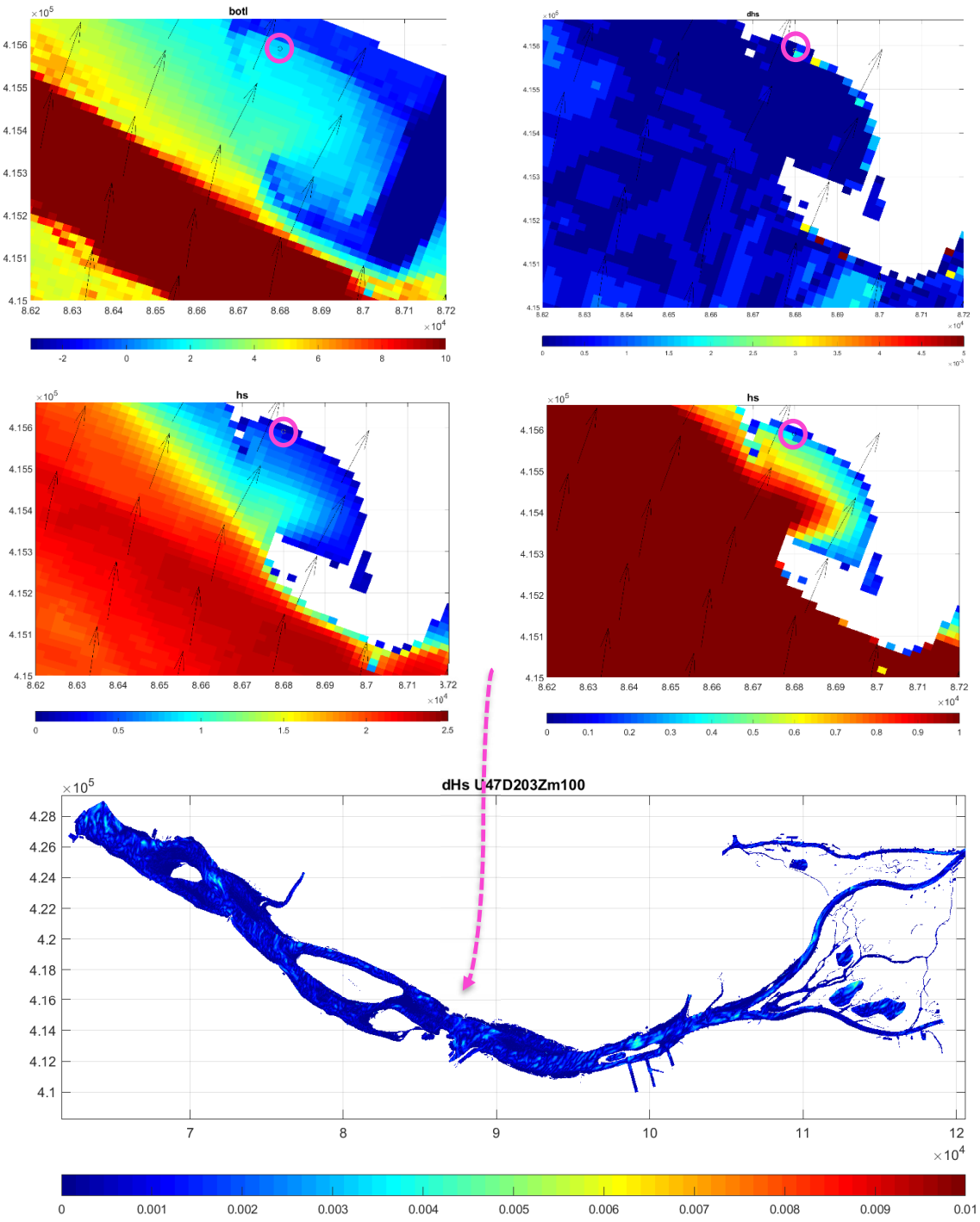

Figure 4.13: Additional plots to check convergence near location 2 (indicated by round pink marker) for run U47D203Zm100. Upper left: Bed level [m-NAP]; upper right: dHs [m]; second row left: H_{m0} [m]; second row right: H_{m0} [m], color scale focussing on location 2; lower panel: dHs [m]

The swan-hvbb computations were carried out on one core only since parallelisation was an issue. The computational time for the high water level runs is approximately 18 hours both on the H6 cluster at Deltares and on the NWM-computational cluster.

5 Brief comparison with a case of WBI 2017

The report Deltares (2016) describing the model set up of the SWAN-model for WBI2017, includes some plots which we can use to compare our new model results with. This provides not more than merely a global visual check to find out what the combined effect of the updated bathymetry and obstacle, the recent SWAN-version and the different model settings is. It is not within the scope of the present study to further analyse the differences.

For the case hvbbU32D270Zp200 (potential wind 32 m/s (applied open water wind U_{10}=31.7 m/s) from 270°N and a water level of NAP+2.00 m), the original and new results are presented below. Note that the colorbars are not identical but close. The results are quite alike although not exactly the same. In the upper river branch (Beneden Merwede), the significant wave height is slightly less now than as computed in Deltares (2016). Furthermore, in the present model schematisation much more obstacles are present.

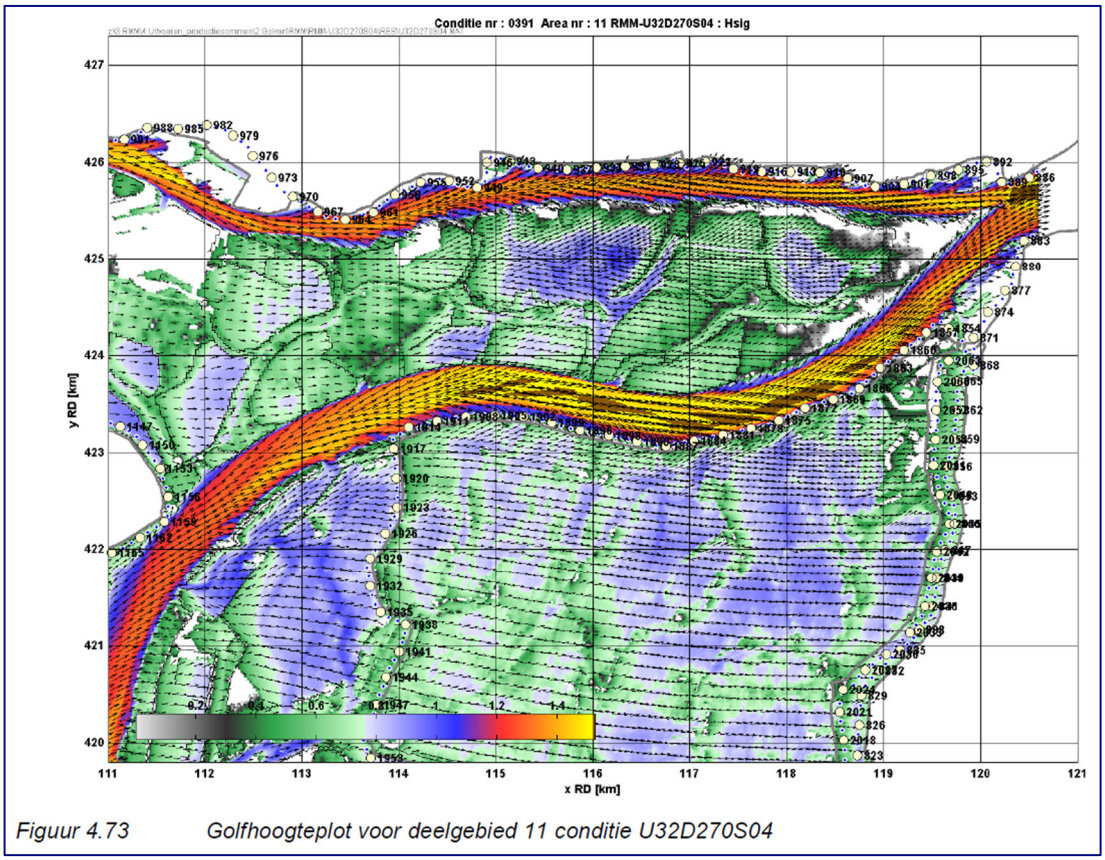

Figuur 4.73 Golfhoogteplot voor deelgebied 11 conditie U32D270S04

Figure 5.1: Results significant wave height [m] run U32D270S04, source: Deltares (2016)

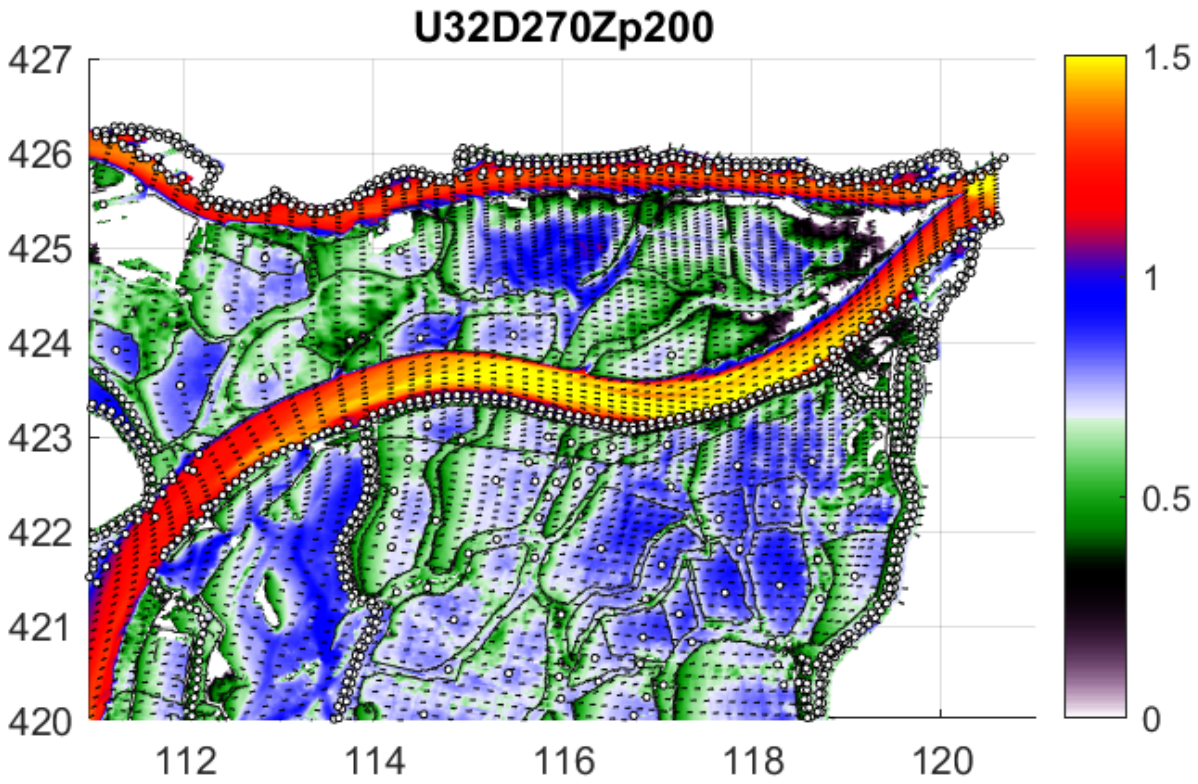

Figure 5.2: Results significant wave height [m] run U32D270Zp200 of the present study (X en Y in km RD-coordinates)

6 Conclusions and recommendations

We set up a SWAN model of the Haringvliet-Biesbosch called swan-hvbb-hr2023_6-v1a, based on baseline-vzm-hr2023_6-v1.

The domain covers (from west to east) the Haringvliet, the wide Hollands Diep, the Biesbosch tidal area and the Noordwaard polder. The curvilinear computational grid is taken from Deltares, 2016. Manual adjustments were made on the bathymetry and obstacles files. The directional resolution is 5°.

The model uses SWAN version 41.31A.1 and uses the generic settings as recommended in Deltares, 2021a,b, such as wind growth and whitecapping according to Van der Westhuysen, shallow water breaking according to Van der Westhuysen and the LTA-OCA triad formulation. For the wind drag we use the Wu formulation in which a fixed value of Cd=0.00275 is used above 30 m/s. Each computation goes through 80 iterations. The model uses uniform wind and water level fields. Flow is not imposed.

Sixteen test computations were performed for the combinations of high and low wind speed (47 m/s and 10 m/s), high and low water level (NAP+7 m and NAP-1 m) and four directions (67.5°N, 202.5° N, 270°N, 315°N). The computations did not reveal anything notable.

There are no measurements available to validate the model. The results look logical and show no abnormalities. . The comparison between the present results and the WBI-2017 results for one testcase (hvbbU32D270Zp200) shows that they are quite close to each other but at some locations (like the Beneden Merwede) the new computed wave heights are a few decimetre smaller.

The model is suitable to use for BOI production computations.

7 Literature

Deltares (2016). SWAN productieberekeningen Rijn-Maasmonding WBI2017 dd 27 June, 2016. Ref 1220082-001-HYE-0011 (M.D. Klein and M.Westra).

Deltares (2020a). Generieke methode voor SWAN modellering for BOI en andere RWS toepassingen. Deltares report 11205758-041-GEO-0001, October 2020 (J. Groeneweg and C. Gautier)

Deltares (2020b). Development sixth-generation model schematization D-HYDRO Volkerak - Zoommeer. Deltares report 11205259-007-ZKS-0008, December, 2020 (Marlies van der Lugt, Luuk van der Heijden, Arjen Markus and Meinard Tiesen).

Deltares (2021a). Instellingen voor SWAN modellen meren en benedenrivieren. Deltares report 11206818-025-GEO-0001, March 2021 (J. Groeneweg).

Deltares (2021b). Vergelijking SWAN brekerformuleringen. Deltares report 11206818-035-GEO-0001, 3 June 2021 (M. Doeleman , J. Groeneweg and J. van Nieuwkoop).

Deltares (2021c). Setup structure G6 repository. Deltares memo 11206814-002-ZKS-0001, CONCEPT, 21 April 2021 (D. Kerkhoven).

Deltares (2021d). SWAN model Veluwerandmeren. Deltares report 11206813-014-ZWS-0002 dated 17 May 2021 (J. van Nieuwkoop).

Deltares (2021e). SWAN-model Volkerak-Zoommeer t.b.v. BOI2023. Deltares report 11206814-006-ZKS-0002 dated 30 September 2021 (Menno de Ridder, Caroline Gautier).

Deltares (2021f). SWAN modelschematisatie Markermeer t.b.v. BOI en RWsOS. Deltares report 11206813-013-ZWS-0001 dated 1 October 2021 (Menno de Ridder, Caroline Gautier).

Deltares (2021g). SWAN-model Greveligen t.b.v. BOI2023. Deltares report 11206814-006-ZWS-0003 dated 7 October 2021 (Madelief Doeleman, Joana van Nieuwkoop).

Eldeberky , Y. (1996). Nonlinear transformation of wave spectra in the nearshore zone (Ph. D. thesis). Netherlands: Delft University of Technology, Department of Civil Engineering.

Rijkswaterstaat (2021). Uitgangspunten Hydraulische Belastingen BOI voor 2023, Beoordelings- en Ontwerp Instrumentarium (BOI). RWS document version 0.9c CONCEPT, April 6, 2021.

Rijkswaterstaat (2022). Instellingen en controles SWAN Haringvliet-Biesbosch t.b.v. de productieberekeningen Rijn- en Maasmonding BOI2023 dd 19 January 2022. Versie V1.1 (P.Oosterlo).

Salmon , JE, Smit, PB, Janssen, TT, & Holthuijsen , LH (2016). A consistent collinear triad approximation for operational wave models. Ocean Modelling, 104, 203-212.

Stijnen, J., T. Botterhuis, M. Benit and C. Gautier (2021). Update Stochasten BOI2023. Memo PR4440.10, dated May 7, 2021 (draft)

Van der Westhuysen, A.J., Zijlema, M., & Battjes, J.A. (2007). Nonlinear saturation based whitecapping dissipation in SWAN for deep and shallow water, coastal engineering, Vol 54, 15-170

Van der Westhuysen, A.J. (2010). Modeling of depth-induced wave breaking under finite depth wave growth conditions, Journal of Geophysical Research, Vol 115, C01008, doi:10.1029/2011JCoo7837.

SWAN team (2020). SCIENTIFIC AND TECHNICAL DOCUMENTATION SWAN Cycle III version 41.31A. Technisch rapport. 29 mei 2020.

Wu, J. (1982). Wind - stress coefficients over sea surface from breeze to hurricane. Journal of Geophysical Research: Oceans, 87(C12), 9704-9706.

A SWAN input

```
$************************ hvbbU10D068Lm100 ************************

$ Model                              : swan-hvbb-hr2023_6-v1a
$ Gebied                             : haringvliet-biesbosch
$ Windsnelheid U10 voor SWAN         : 10.00 m/s
$ Windrichting                       : 67.50 gr
$ Waterstand t.o.v. N.A.P.           : -1.00 m
$ Variant                            :  a
$ template opgesteld voor SWAN-versie 41.31.A1 dd feb 2022 t.b.v. BOI

$*************************************************************

PROJECT 'HR2023' 'hvbb'

$------------- algemeen -----------

SET     LEVEL=-1.00 MAXERR=2 RHO=1000 CDCAP=0.00275 NAUTICAL
MODE    STATIONARY TWODIMENSIONAL
COORDS  CART

$------------- invoer -----------

CGRID CURVILINEAR  907 3424 EXCE 0.0  0.0 CIRCLE 72  FLOW=0.06
FHIGH=2.4
READ  COORD 1. '../../../geometry/hvbb-hr2023_6-v1a.grd' IDLA=6
NHEDF=0  NHEDVEC=1 FREE

INP   BOTTOM CURVILINEAR 0. 0. 907 3424 EXCE 999.000
READ  BOTTOM -1. '../../../geometry/hvbb-hr2023_6-v1a.bot' IDLA=5
NHEDF=0 FREE

WIND  10.00    67.50  DRAG  WU

INCLUDE '../../../geometry/hvbb-hr2023_6-v1a.fxw'

$------------- fysica & numeriek -----------

GEN3  WESTH
WCAP  WESTH      CDS2=5.0e-05 BR=0.00175   P0=4.0    POWST=0.0
POWK=0.0 NLDISP=0.0 CDS3=0.8 POWFSH=1.0
QUAD  IQUAD=2    LAMBDA=0.25  CNL4=3.0e+07 CSH1=5.5  CSH3=-1.25
BREA  WESTH      ALPHA=0.96  POWN=2.5 BREF=-1.39630 SHFAC=500.0
FRIC  JONSWAP    CFJON=0.038
TRIAD itriad=11  TRFAC=0.1 CUTFR=2.5

NUMERIC STOPC     DABS=0.005 DREL=0.01 CURVAT=0.001 NPNTS=101 STAT
MXITST=80 ALFA=0.001
```

```
$------------ uitvoer -----------

BLOCK   'COMPGRID'  NOHEAD  'results/hvbbU10D068Lm100.nc' LAY-OUT 3 &
         XP YP BOTLEV HSIG TPS RTP TMM10 TM01 TM02 DIR DSPR PDIR DHS
DRTM01 WATLEV WIND WLEN UBOT URMS

POINTS 'p7' FILE '../../../geometry/output_locations/swan-hr2023-
p7.xyn'
TABLE  'p7' HEAD 'results/hvbbU10D068Lm100_p7.tab' XP YP DEP HSIG TPS
TMM10 TM01 TM02 &
      DIR DSPR DHS DRTM01 WATLEV WIND WLEN FORCE UBOT

SPEC   'p7' SPEC1D ABS 'results/hvbbU10D068Lm100_p7.sp1'
SPEC   'p7' SPEC2D ABS 'results/hvbbU10D068Lm100_p7.sp2'

TEST  1 0 POINTS XY    79451     419304 &
       77756     415633 &
       65638     427677 &
       64485     425488 &
       86806     415593 &
       85315     413082 &
       108594    418210 &
       109103    414767 &
       116533    413541 &
       118108    418220 &
       111495    422231 &
       104731    417845 &
       101458    414859 &
       81924     418541 &
       79880     414727 &
       76722     416668 &
       63269     426305 &
       65284     428041 &
       71634     424942 &
       111456    414998 &
       71212     421593 &
       93754     413575 &
       91812     411057 &
       103025    413941 PAR 'results/hvbbU10D068Lm100.tst'
       S1D 'results/hvbbU10D068Lm100.s1d' &
       S2D 'results/hvbbU10D068Lm100.s2d'

COMPUTE STATIONARY
STOP
```

B Figures

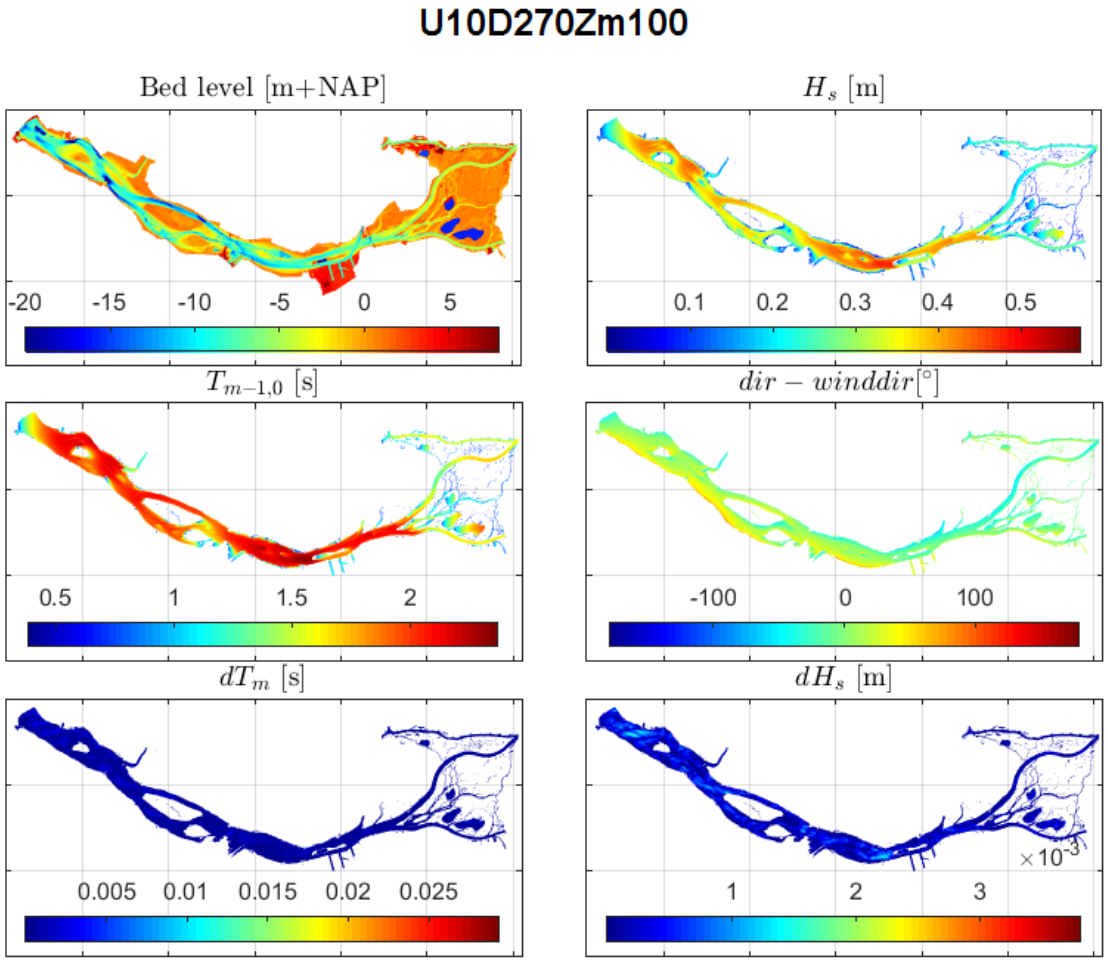

Figure B-1 Results U10D270Zm100 (10m/s wind from 270°N, water level -1m+NAP)

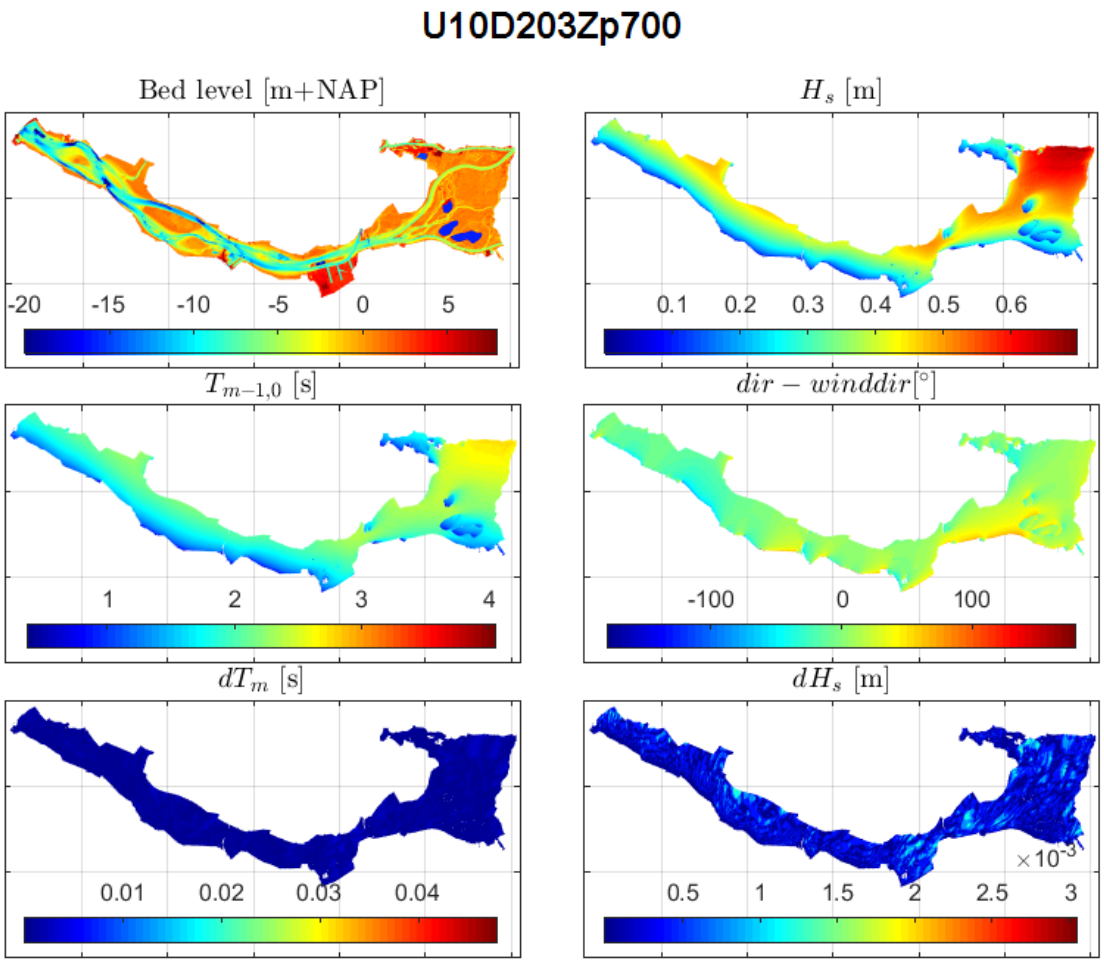

Figure B-2 : Results U10D203Zp700 (10m/s wind from 202.5°N, water level 7m+NAP)

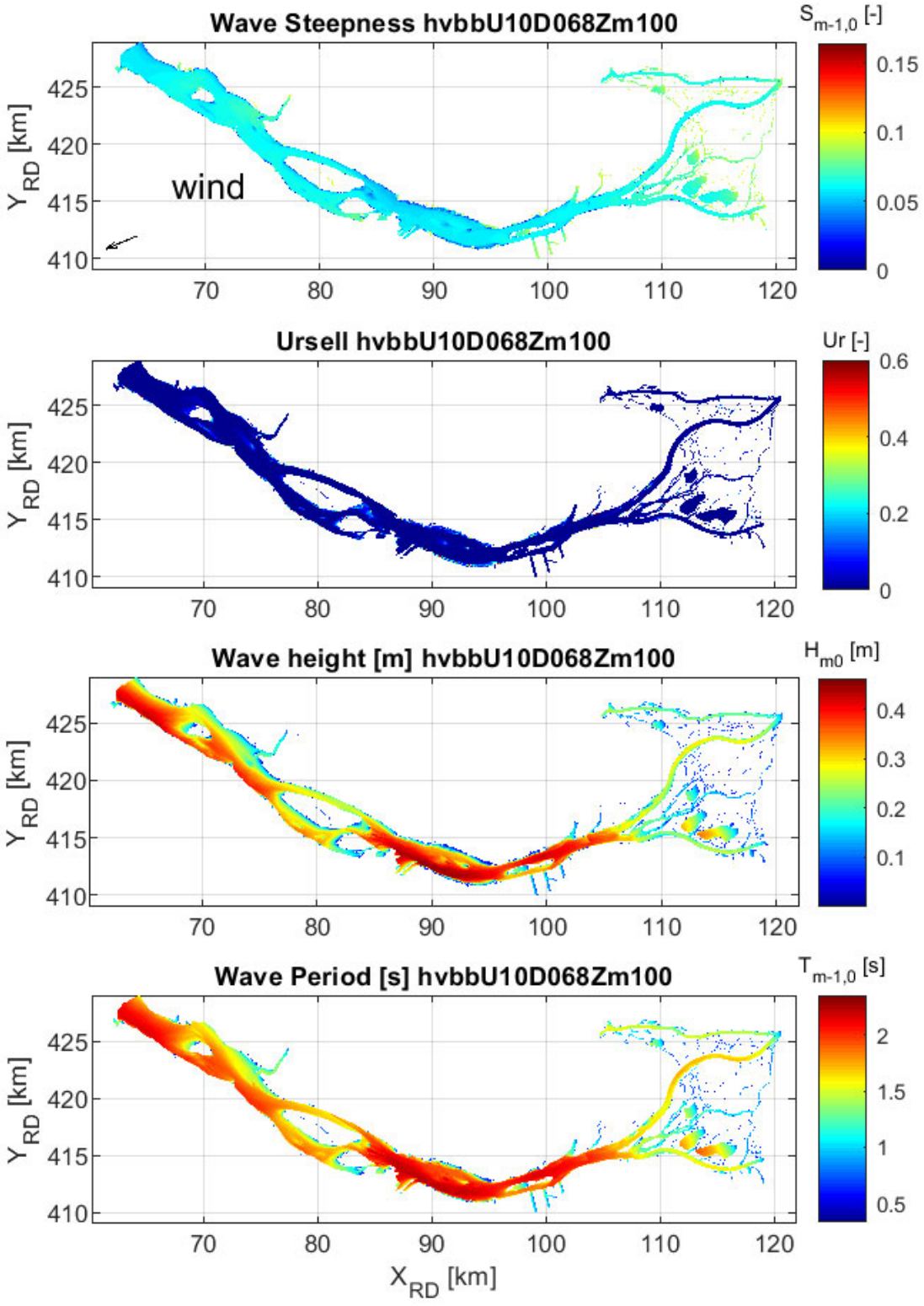

Figure B-3 : Results Wave Steepness, Ursell number, H_{m0} en $T_{m-1,0}$

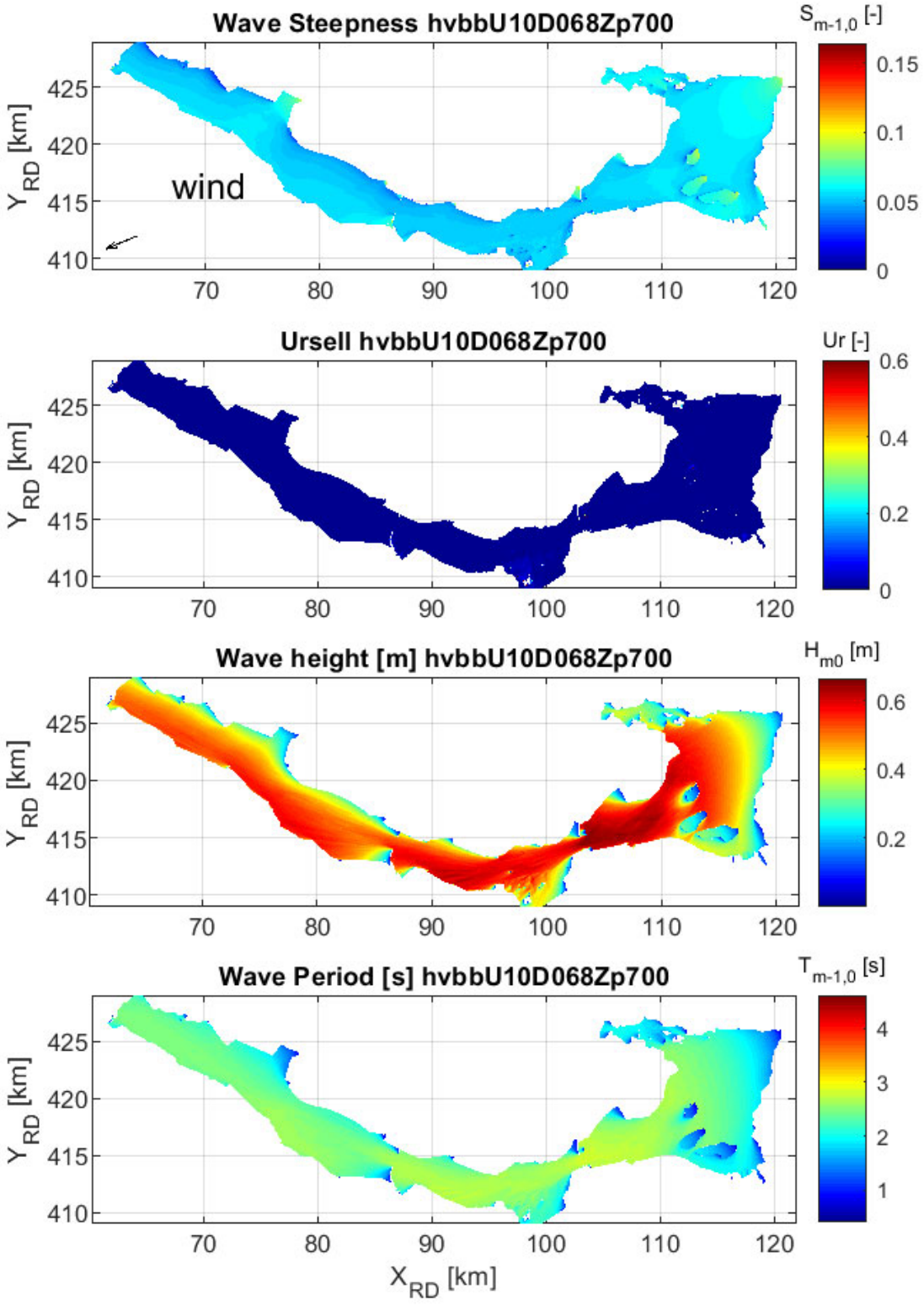

Figure B-4 : Results Wave Steepness, Ursell number, H_{m0} en $T_{m-1,0}$

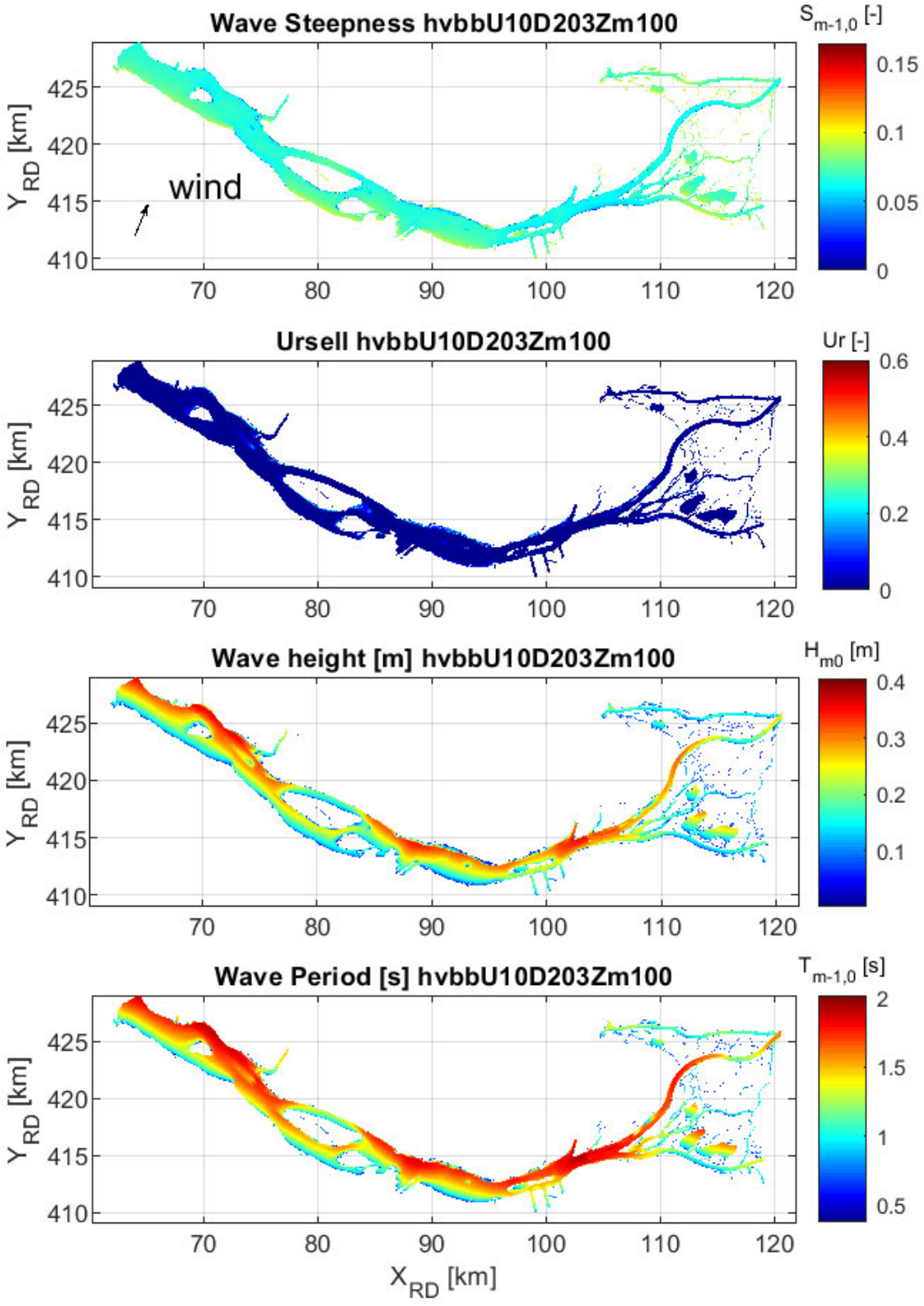

Figure B-5 : Results Wave Steepness, Ursell number, H_{m0} en $T_{m-1,0}$

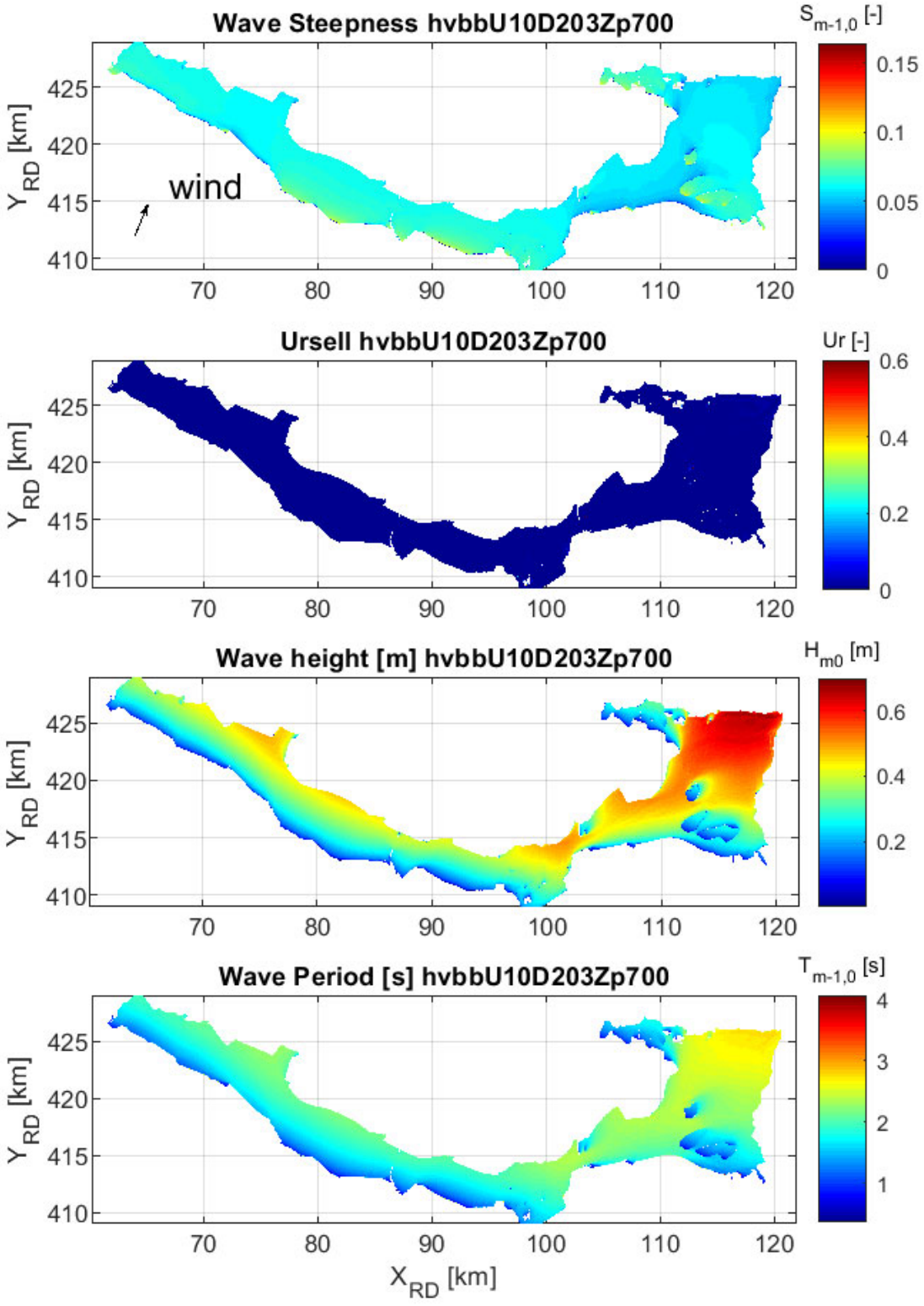

Figure B-6 : Results Wave Steepness, Ursell number, H_{m0} en $T_{m-1,0}$

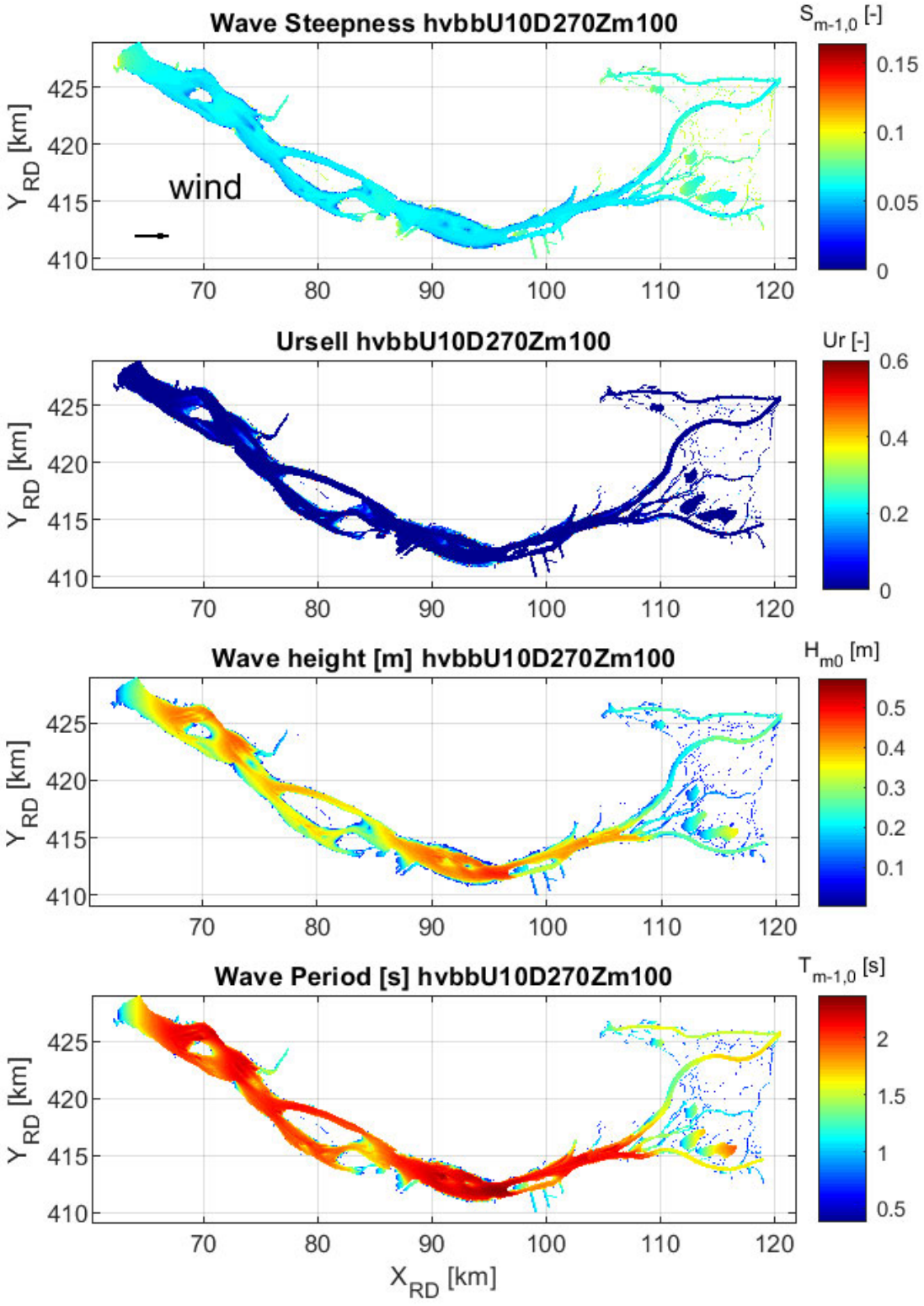

Figure B-7 : Results Wave Steepness, Ursell number, H_{m0} en $T_{m-1,0}$

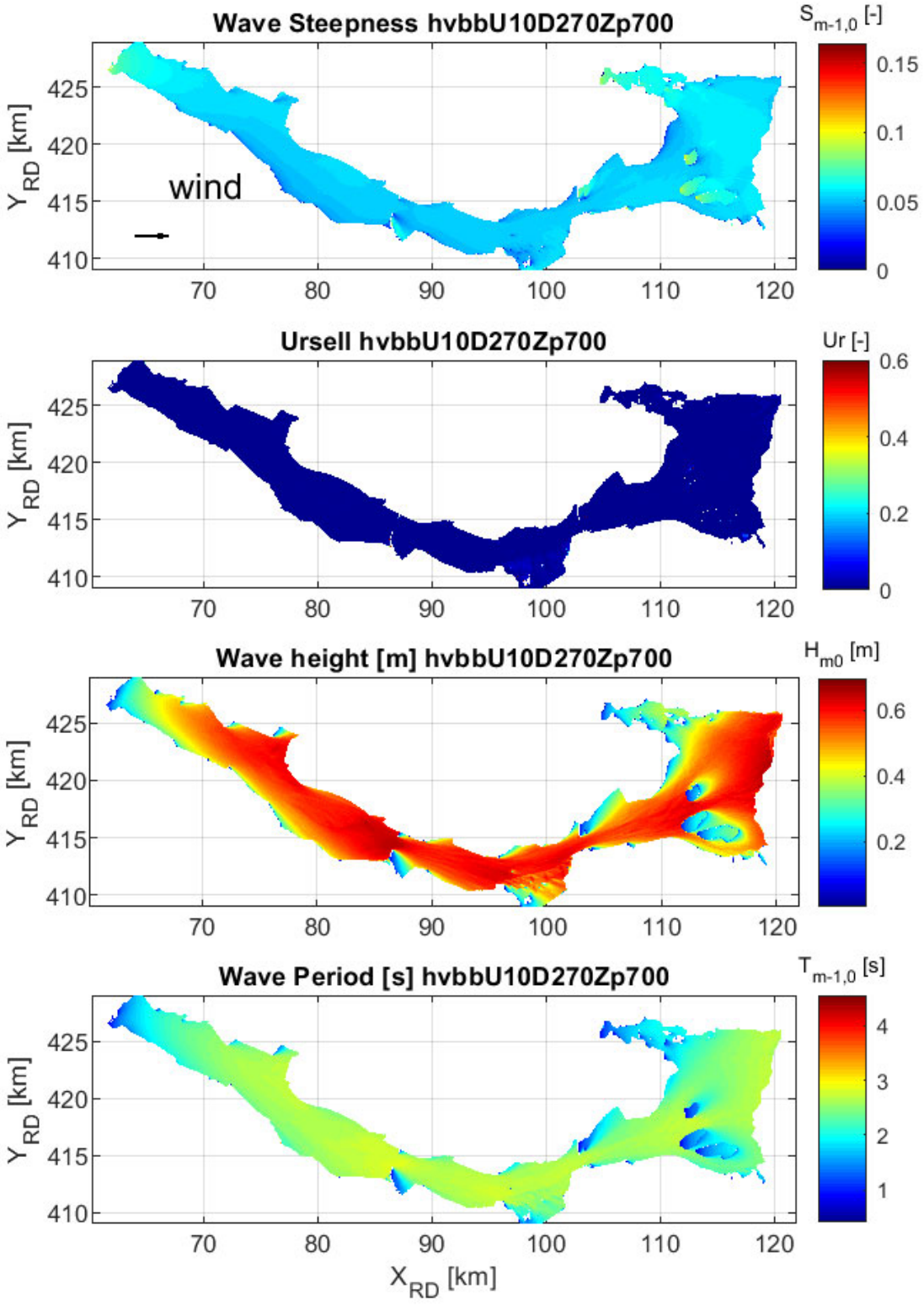

Figure B-8 : Results Wave Steepness, Ursell number, H_{m0} en $T_{m-1,0}$

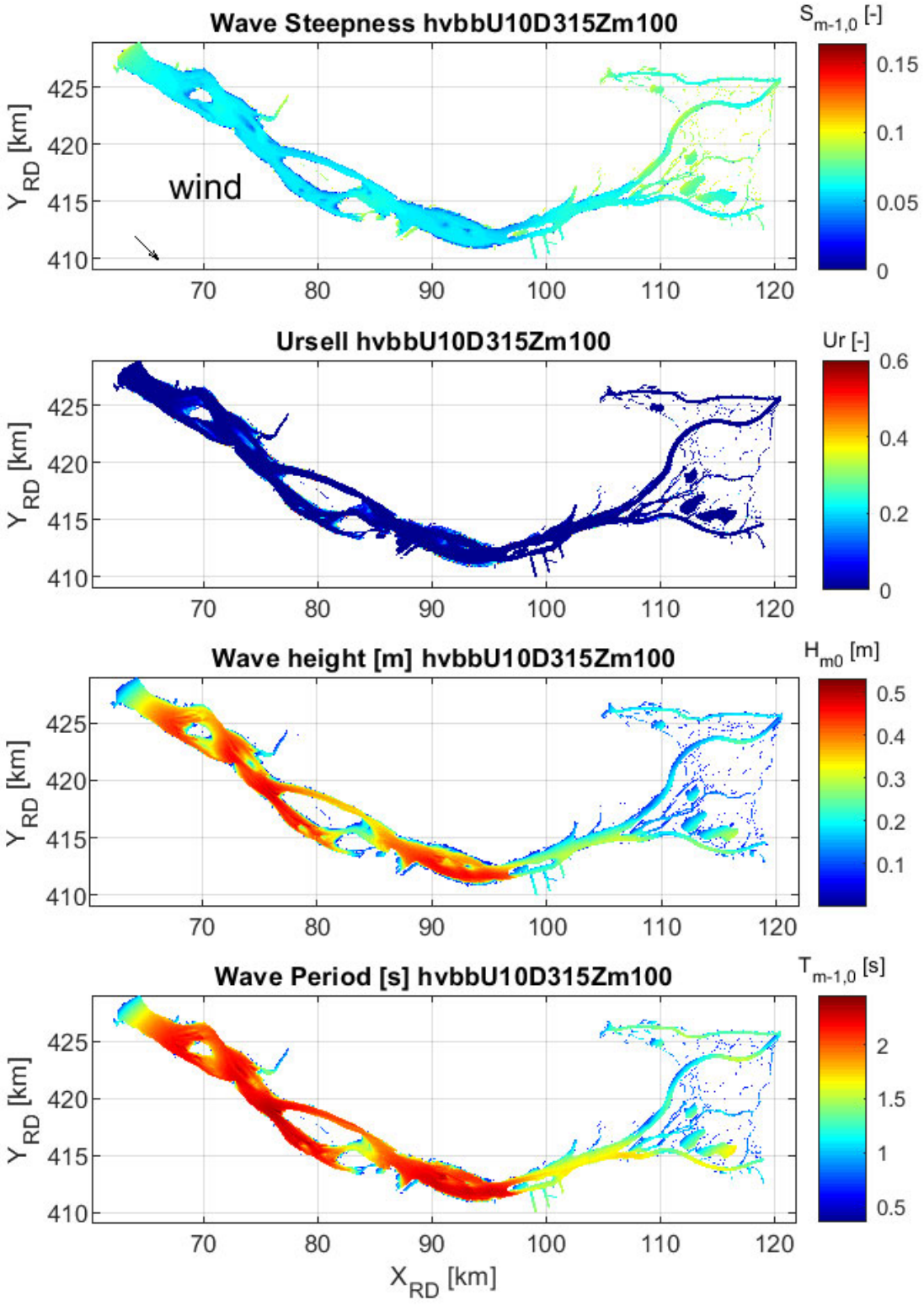

Figure B-9 : Results Wave Steepness, Ursell number, H_{m0} en $T_{m-1,0}$

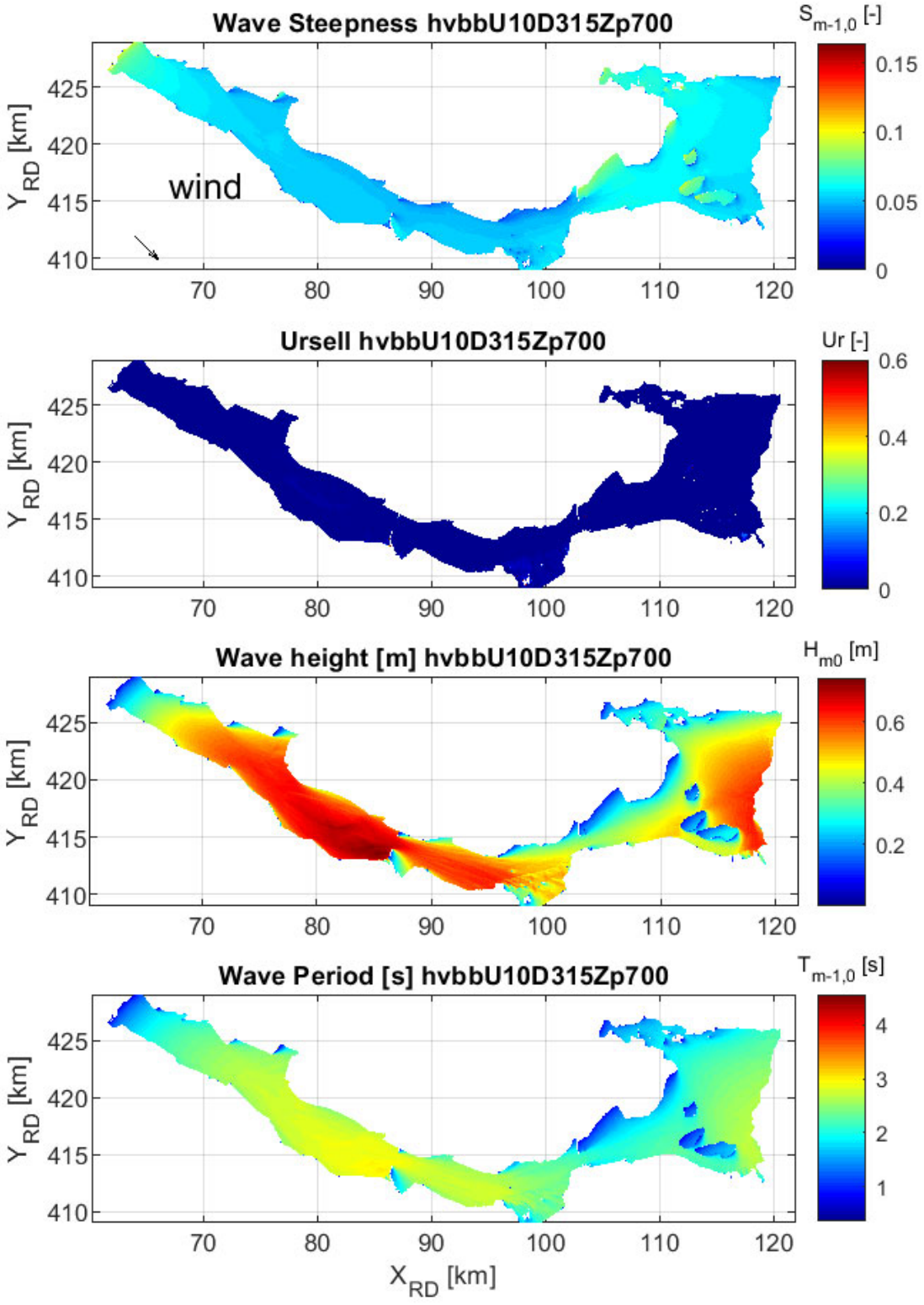

Figure B-10 : Results Wave Steepness, Ursell number, H_{m0} en $T_{m-1,0}$

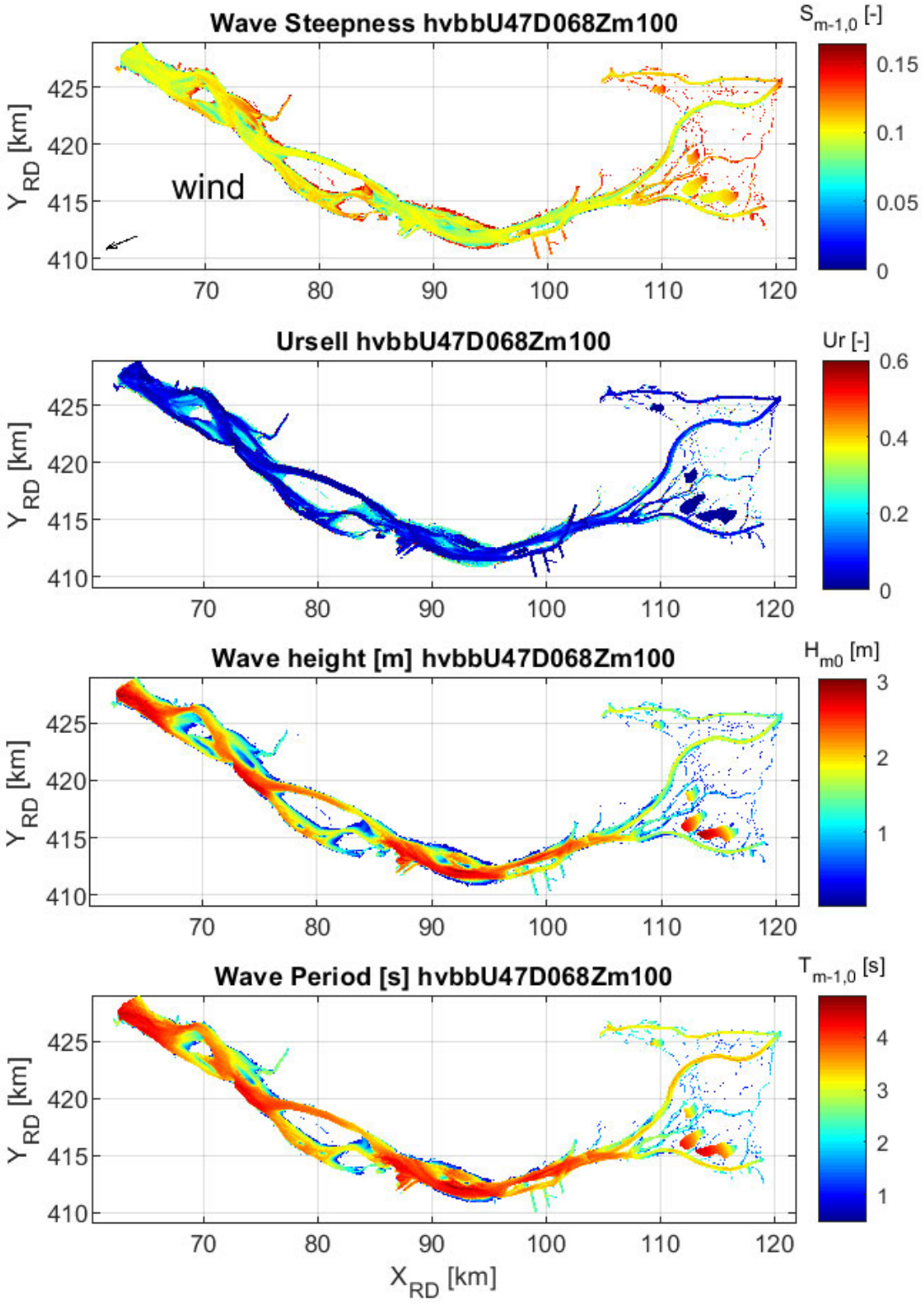

Figure B-11 : Results Wave Steepness, Ursell number, H_{m0} en $T_{m-1,0}$

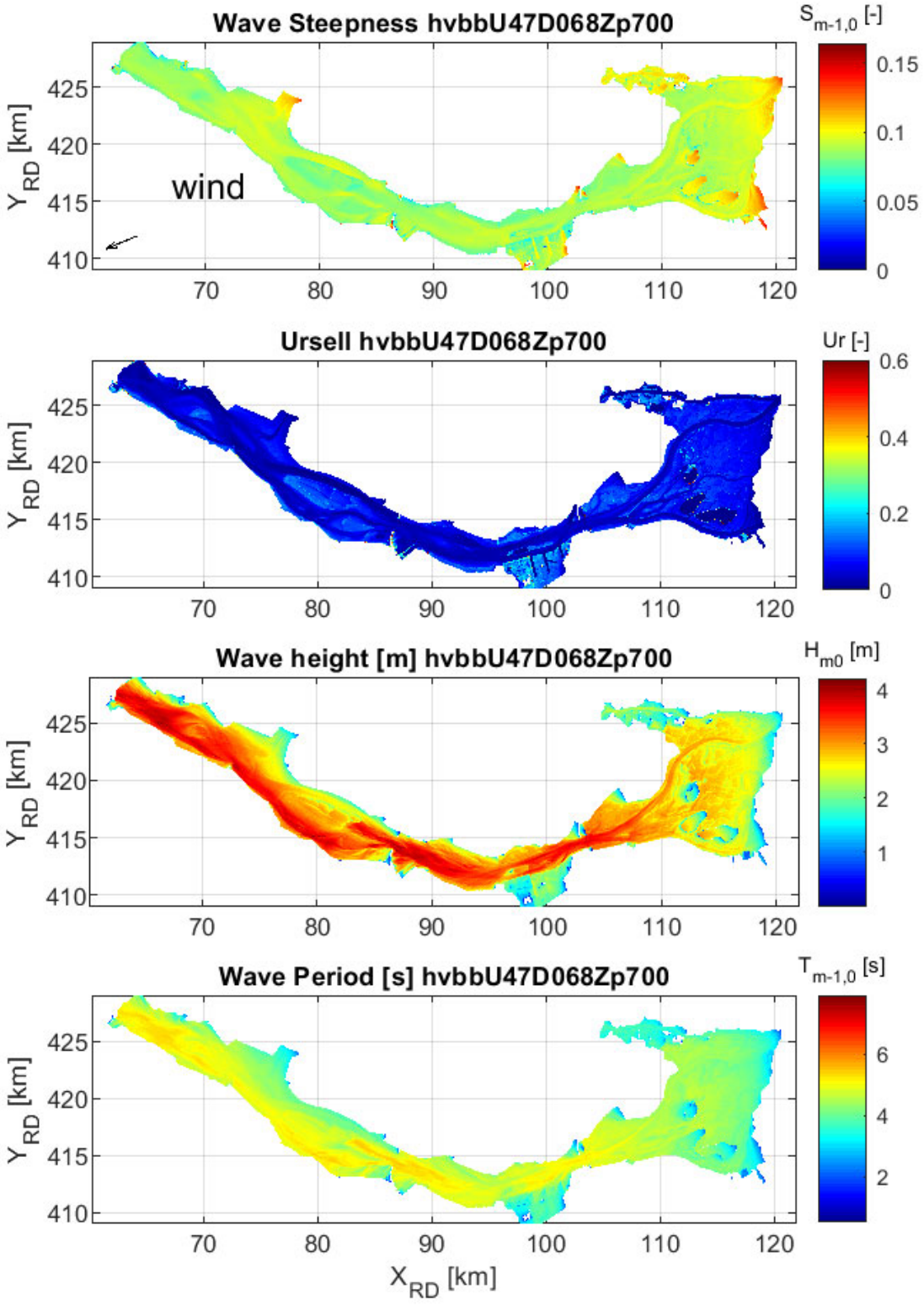

Figure B-12 : Results Wave Steepness, Ursell number, H_{m0} en $T_{m-1,0}$

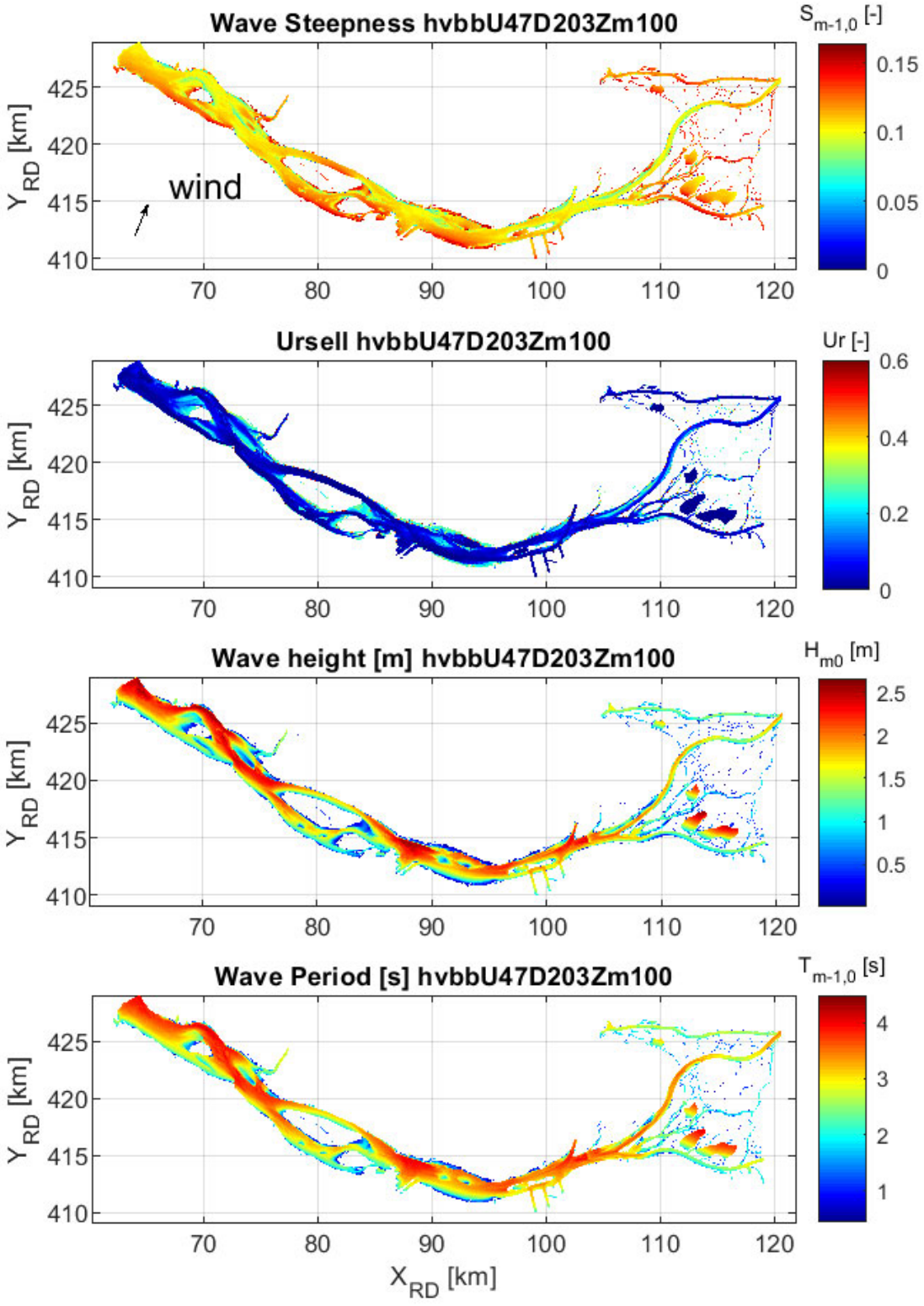

Figure B-13 : Results Wave Steepness, Ursell number, H_{m0} en $T_{m-1,0}$

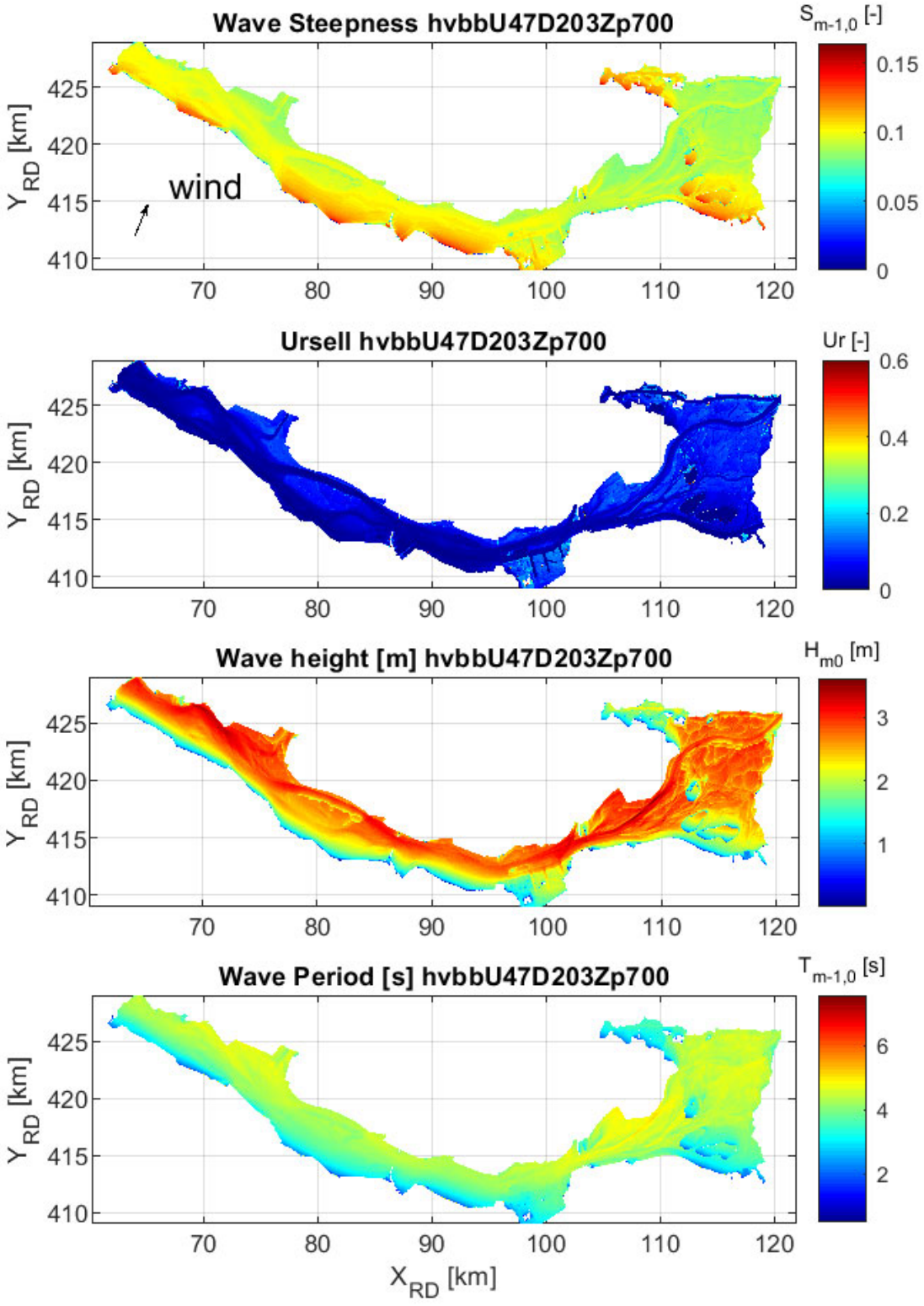

Figure B-14 : Results Wave Steepness, Ursell number, H_{m0} en $T_{m-1,0}$

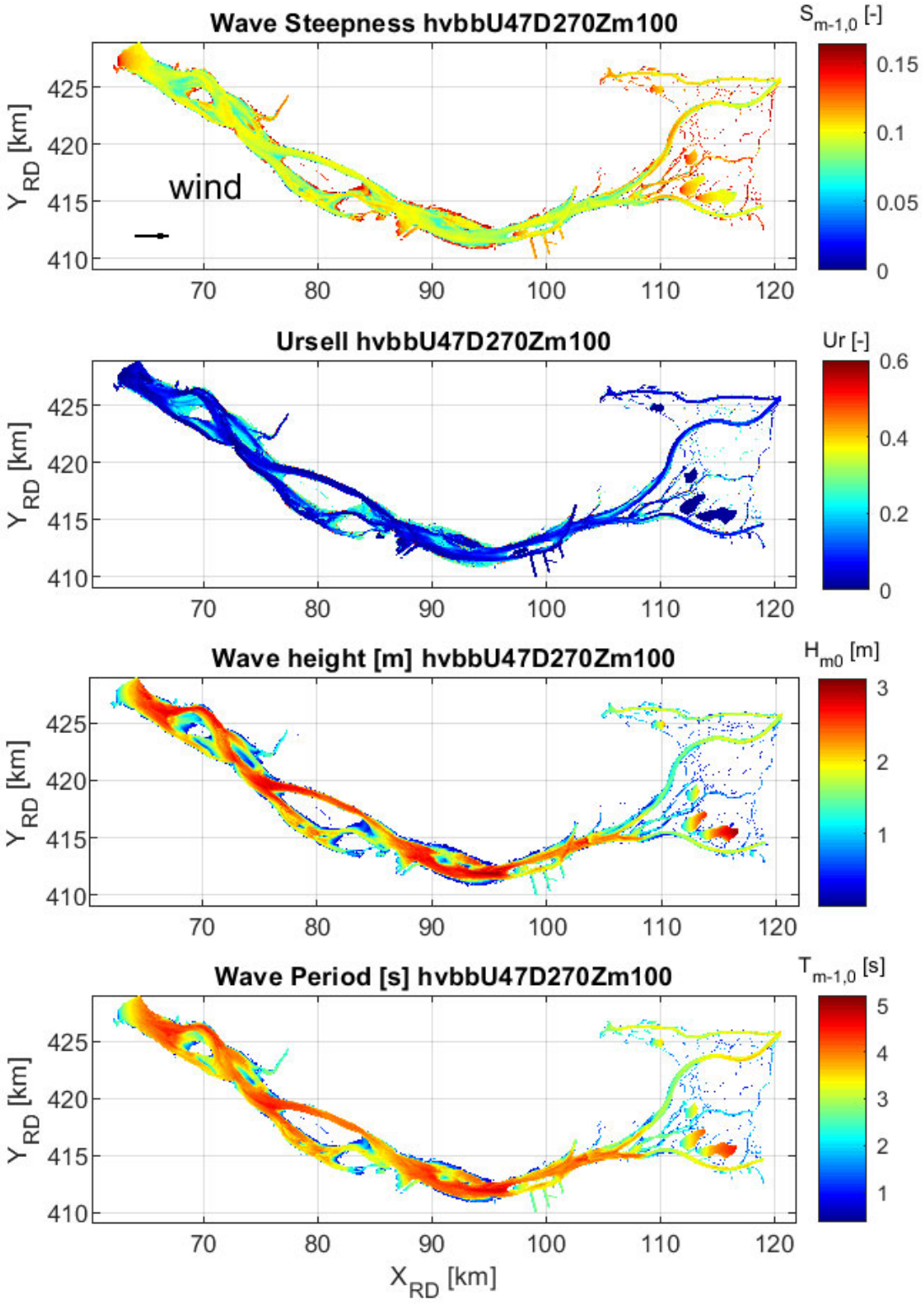

Figure B-15 : Results Wave Steepness, Ursell number, H_{m0} en $T_{m-1,0}$

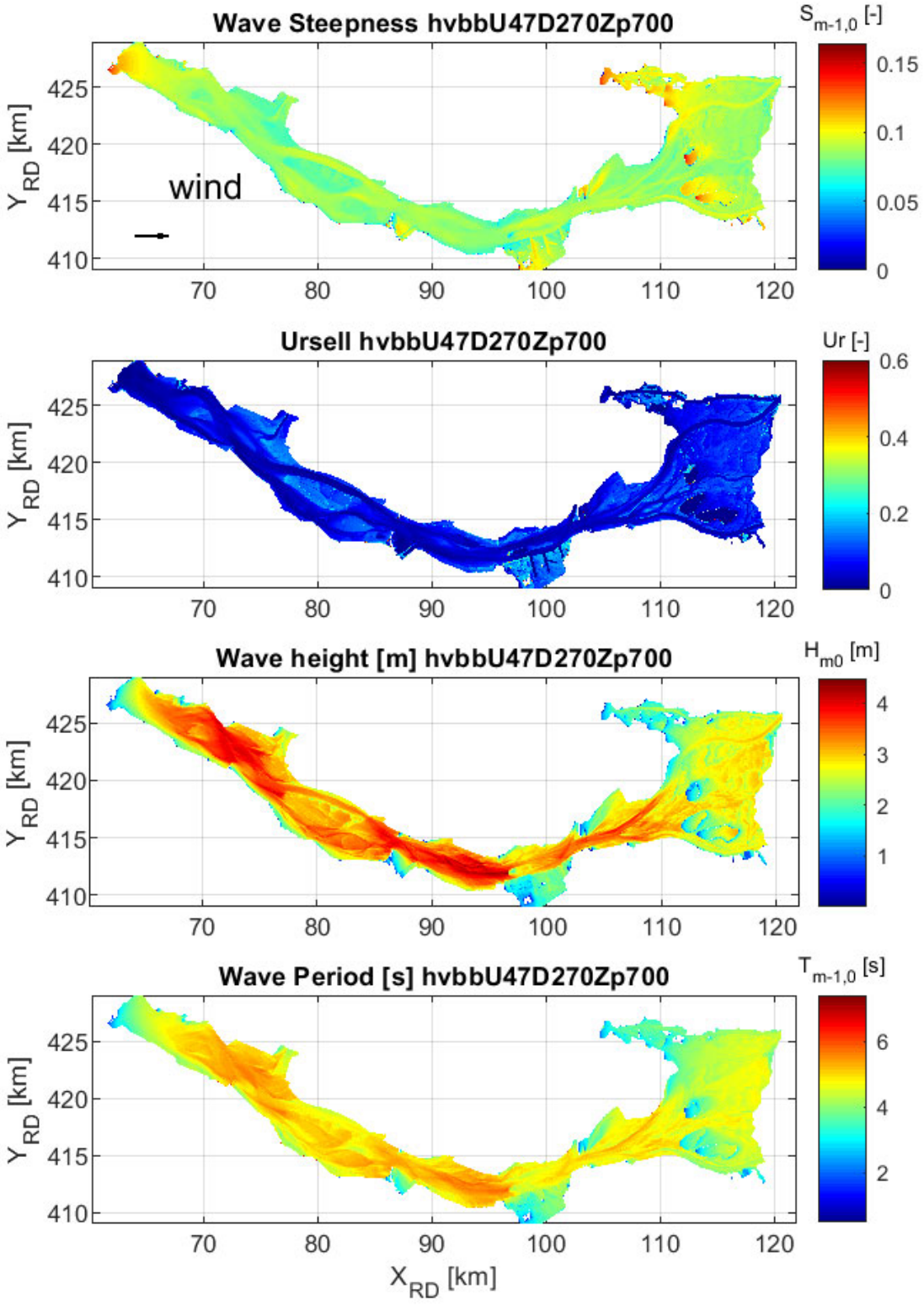

Figure B-16 : Results Wave Steepness, Ursell number, H_{m0} en $T_{m-1,0}$

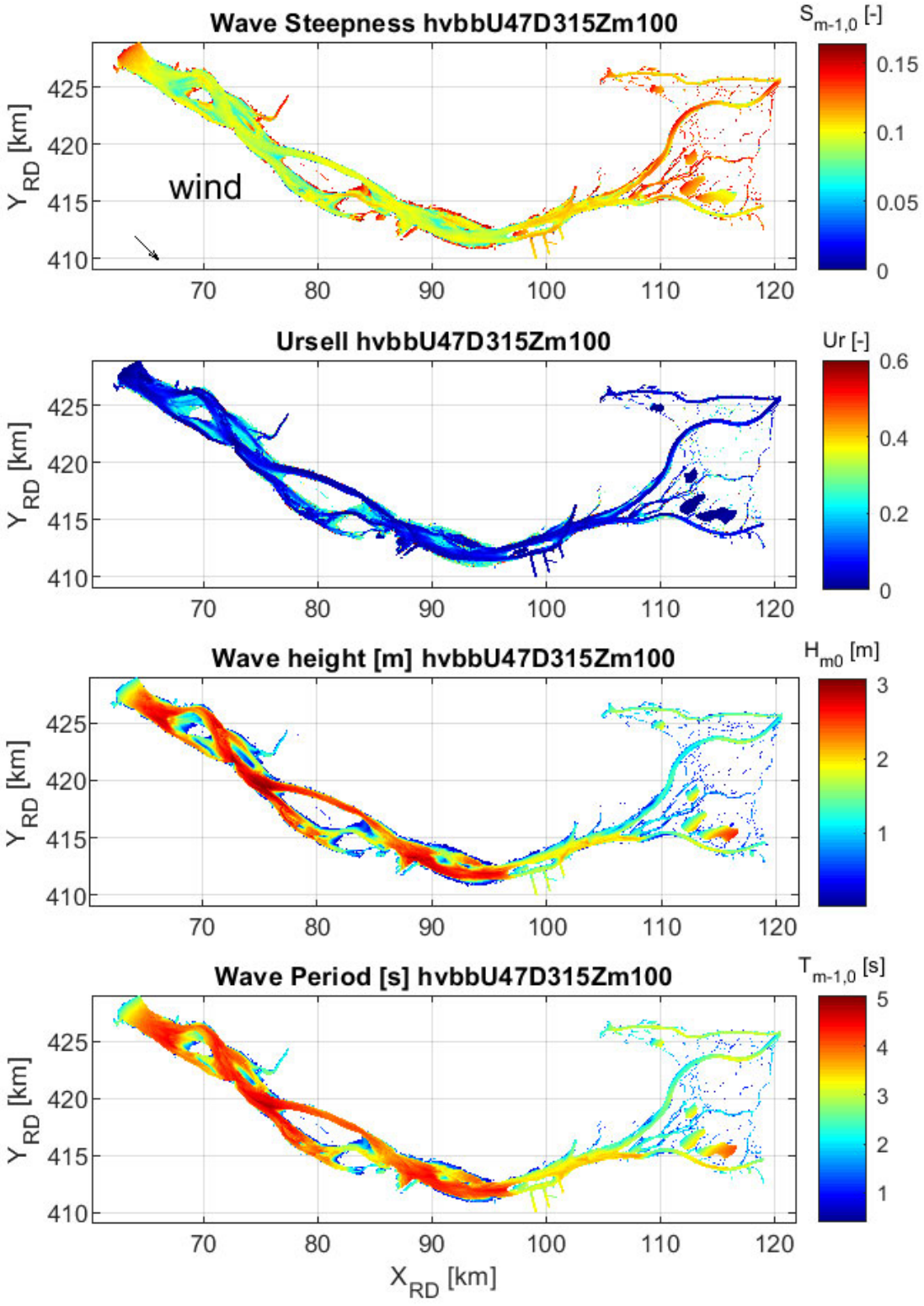

Figure B-17 : Results Wave Steepness, Ursell number, H_{m0} en $T_{m-1,0}$

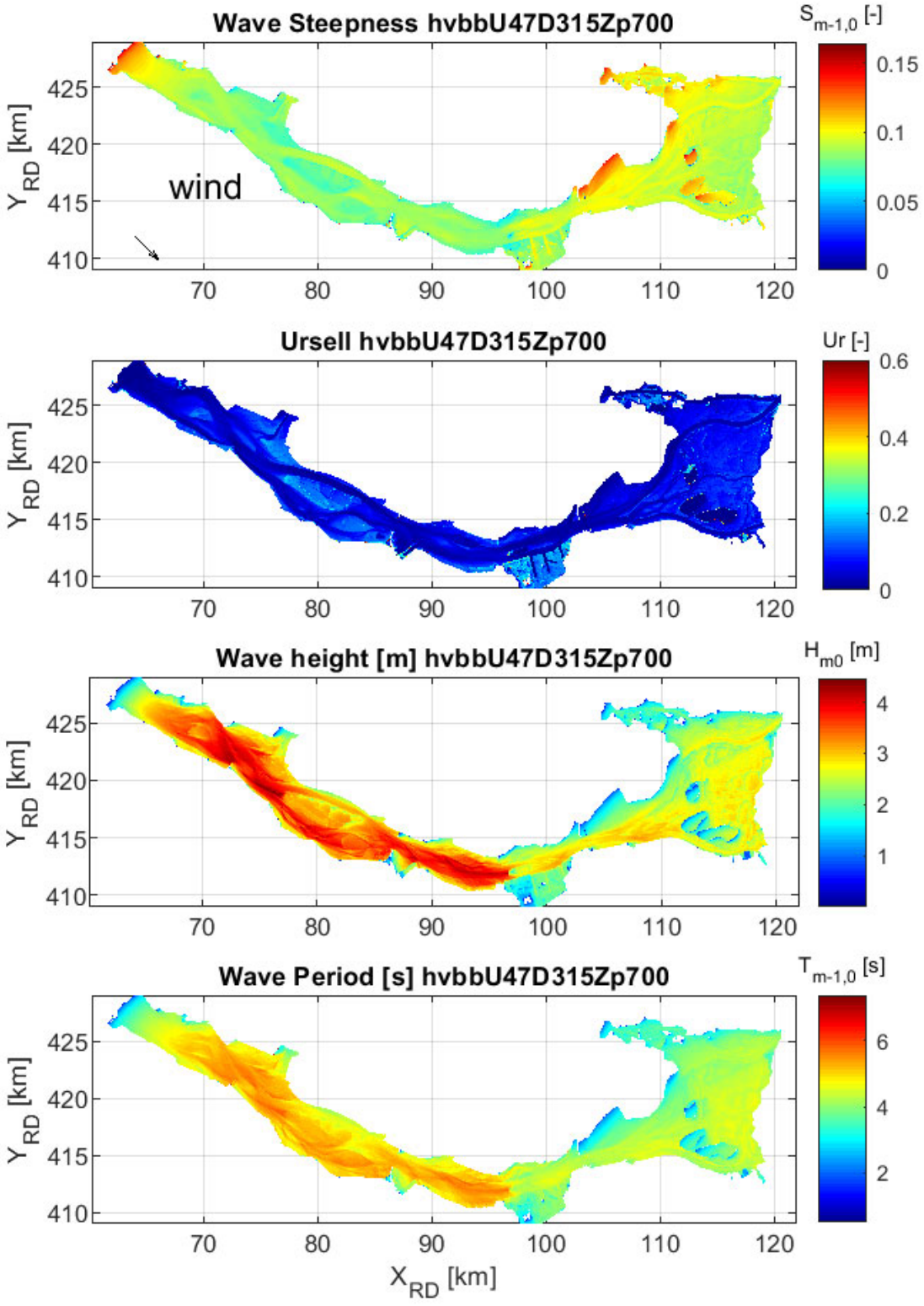

Figure B-18 : Results Wave Steepness, Ursell number, H_{m0} en $T_{m-1,0}$

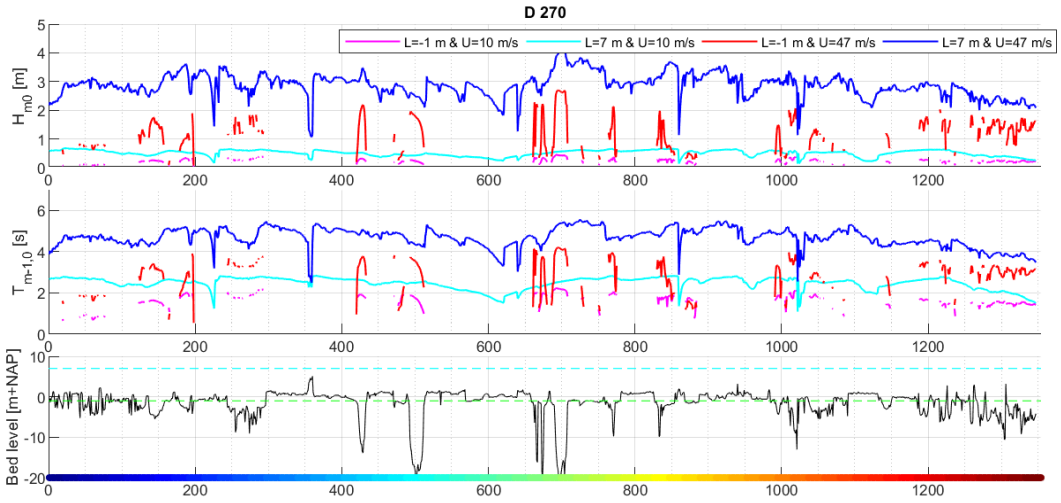

Figure B-19 SWAN results of wave height (upper panel), wave period (middle panel) and bed level (lower panel) at the output points for four runs with a wind direction of 270°N. The color band in the lower panel matches the locations shown in Figure 4.5. The green dotted line represents NAP-1 m and the cyan dotted line indicates NAP+7 m.

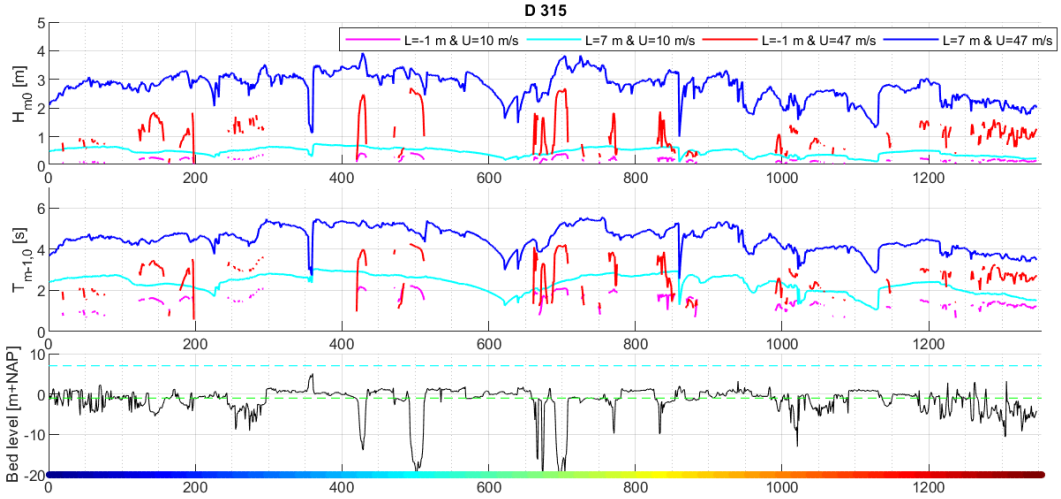

Figure B-20 SWAN results of wave height (upper panel), wave period (middle panel) and bed level (lower panel) at the output points for four runs with a wind direction of 315°N. The color band in the lower panel matches the locations shown in Figure 4.5. The green dotted line represents NAP-1 m and the cyan dotted line indicates NAP+7 m.

Deltares is een onafhankelijk kennisinstituut voor toegepast onderzoek op het gebied van water en ondergrond. Wereldwijd werken we aan slimme oplossingen voor mens, milieu en maatschappij.

Deltares

www.deltares.nl